INTERNATIONAL
Agrophysics
www.international-agrophysics.org

Int. Agrophys., 2026, 40, 469-492
doi: 10.31545/intagr/226373

Determination of the influence of moisture content on various mechanical properties of wood pellets**

Manuel Moya-Ignacio[1]*, *José Ramón Villar-García*[1], *Pablo Vidal López*[2], *Miriam Campo-González*[1]

[1]Department of Ingeniería del Medio Agronómico y Forestal, Universidad de Extremadura, Centro Universitario de Plasencia Avda. Virgen del Puerto nº 2, 10600 Plasencia (Cáceres), Spain
[2]Department of Ingeniería del Medio Agronómico y Forestal, Universidad de Extremadura, Escuela de Ingenierías Agrarias, Avda. Adolfo Suárez, s/n. 06007 Badajoz, Spain

Received April 30, 2026; accepted July 24, 2026

A b s t r a c t. In recent years, the demand for wood pellets has increased worldwide. Moreover, its production is rising and the number of facilities to store them is increasing as well. Since this product is usually stored in agricultural silos, the loads generated inside them depend on its mechanical properties. Therefore, the purpose of this research was the determination of some mechanical properties such as the angle of internal friction, the apparent cohesion, the dilatancy angle, the grain-wall friction coefficient, or the specific weight of wood pellets subjected to different moisture contents. The main findings of this study were that no correlation was found between the moisture content of the wood pellet samples and any of the following parameters: the angle of internal friction, the effective angle of internal friction, the apparent cohesion, the dilatancy angle, or the grain-wall friction coefficient within the moisture range used in this study. Furthermore, the angle of internal friction ranged from 35.7º to 41.4º. Finally, there was a correlation between the apparent specific weight and the moisture content of the sample. These data may be useful to design suitable, efficient, and cost-effective facilities and infrastructure for the handling and storage of biomass products.

K e y w o r d s: wood pellet, mechanical testing, friction, apparent specific weight, moisture

*Corresponding author e-mail: manuelmi@unex.es
**This research was developed within the scope of the R&D Project PID2024-158768NB-I00 ("Flow and breakage of granular particles in steel silos and simulation with Discrete Element Models -SIMUBREAK") funded by MICIU/AEI/10.13039/501100011033 and by ERDF/UE. This paper has been co-financed 85% by the European Union, the European Regional Development Fund and the Regional Government of Extremadura. Managing authority: Ministry of Finance. Grant file numbers: GR24154 and GR24077.

1. INTRODUCTION

As greenhouse gas emissions continue growing, many countries are committed to reduce them. In fact, they are expected to roughly stabilise between 2025 and 2030, even projecting a declining path before 2030 (International Energy Agency, 2025). Furthermore, many experts considered that peaking before 2025 might have been possible but hinged on the acceleration of the energy transition and curbing the supply and demand for fossil fuel (United Nations Environment Programme, 2024). For these reasons, wood pellets are considered a viable alternative to fossil fuels as nations strive to reduce their carbon footprints. At a global level, nowadays the United States of America is the most important producer of wood pellets in the Economic Commission for Europe (ECE) region, whereas Europe and Asia are the most important consumers of this product. The wood pellet market industry is experiencing a surge in demand because of the shift towards renewable energy sources, and the forecast is that it will continue growing during the period 2025-2035. Although in the case of the European Union (EU) the consumption of wood pellets declined in 2023 and 2024 (United Nations Economic Commission for Europe (UNECE), 2025), the forecast for next years is that the demand for wood pellets will grow, although the EU production will not follow that trend due to the limited sustainable supply of woody biomass. Because of this, EU imports are projected to recover although the Deforestation-free Supply Chain Regulation (EUDR) could become a trade barrier in that sense (Flach and Bolla, 2025).

If the trend described above comes true, more storage facilities for wood pellets would be needed in the medium and long term. Stelte (2012) identified the major problems that may arise when large amounts of biomass are handled. They are mainly related to dust formation, off-gassing, self-heating, and biological hazards. In fact, different problems may occur during handling and storage, depending on biomass origin, size, shape, composition, and moisture content.

Since mechanical forces may appear during pellet transportation, they can lead to fractures and breakage of the pellets resulting in fines and dust. Although pellet producers must follow the standards (EN ISO 17225-1, 2022) to achieve high strength and abrasion resistance, this problem cannot be eliminated completely, especially in large scale applications such as heat and power plants, because they usually do not follow these standards (Stelte, 2012).

Mechanical properties of different granular agricultural materials, such as the angle of internal friction, the apparent cohesion, the bulk density, Young's modulus, or the friction coefficient, among others, have been studied for years since the loads generated inside agricultural silos strongly depend on these properties. Most studies have been mainly focused on dry materials under environmental conditions (Lebègue and Boudakian, 1989; Lopes Neto *et al.*, 2016; Molenda and Horabik, 2005; Ramírez *et al.*, 2010; Thompson *et al.*, 1988). However, some studies have been conducted with materials subjected to different moisture contents (Bhise *et al.*, 2014; Davies and El-Okene, 2009; Izli *et al.*, 2009; Kruszelnicka *et al.*, 2022a; Tabatabaeefar, 2003).

These parameters are needed in both traditional silo design methods (Janssen, 1895; Reimbert and Reimbert, 1987) and numerical methods. Among the latter, many studies have been conducted using the finite element method (Doerich and Rotter, 2011; Gao *et al.*, 2018; Hilal *et al.*, 2022; Jofriet *et al.*, 1977; Mohammad *et al.*, 2023), while the application of discrete element models is increasing more recently (Kobyłka *et al.*, 2019; Liu *et al.*, 2017; Markauskas *et al.*, 2015; Molenda *et al.*, 2011; Wiącek *et al.*, 2023), and even a combination of both approaches (Bagherzadeh Kh. *et al.*, 2011; Rotter *et al.*, 1998; Sarnavi *et al.*, 2013; Zheng *et al.*, 2017). The application of these new techniques requires the determination of new parameters (Chen *et al.*, 2020; Gallego *et al.*, 2020; Gierz *et al.*, 2022; Kruszelnicka *et al.*, 2022b; Sarnavi *et al.*, 2013), helping to understand the behaviour of different materials when they are stored inside silos under static or dynamic conditions (Bagherzadeh Kh. *et al.*, 2011; Gallego *et al.*, 2025; Kruszelnicka *et al.*, 2024; Liu *et al.*, 2017; Weinhart *et al.*, 2016).

Several studies have highlighted the importance and influence of moisture content on these parameters, as well as its impact on the loads and type of flow generated inside silos during storage and discharge. Among the effects that changes in moisture content can cause, it is worth noting, for example, variations in the bulk density of granular agricultural materials depending on the grain depth inside silos (Cheng *et al.*, 2017; Gao *et al.*, 2018; Ramaj *et al.*, 2024). Furthermore, their physical and mechanical properties may undergo significant changes (Çarman, 1996; Chandio *et al.*, 2021; Gierz *et al.*, 2022; Kibar and Öztürk, 2008; Zhu *et al.*, 2023). Meanwhile, the flow behaviour of the material can also be affected when the moisture content varies (Ganesan *et al.*, 2008; Lu *et al.*, 2023). Different patterns of wall pressure and stress on cylindrical silos can be observed (Kibar, 2017) or the strength characteristics or failure mode of the material may also be affected (Horabik *et al.*, 2021; Richefeu *et al.*, 2006; Smith and Litster, 2012).

Considering the information provided above, the aim of this work was to determine some mechanical properties of wood pellets when subjected to different moisture contents. Some of these parameters have been previously reported by other authors and therefore they will be compared with their findings. In other cases, new data will be provided to the literature. All these parameters can be useful for the optimisation of handling and storage structures.

2. MATERIALS AND METHODS

The Geotechnical Laboratory in the Centro Universitario de Plasencia (University of Extremadura) was the place where the authors performed all the tests reported in this work. The material used was wood pellet, which corresponded to natural wood (100%). It was provided by the company Coterram, located in the province of León (Spain). The main characteristics of this material were as follows: diameter = 6 ± 1 mm, length = 3.15 < L ≤ 40 mm, fines ≤0.5%, net calorific value ≥ 4.6 kWh kg^{-1}, ash ≤ 0.7%, moisture ≤ 10%, bulk density = 600 ≤ DB ≤ 750 kg m^{-3}, mechanical durability ≥ 98%.

The material properties determined in this research were the angle of internal friction (φ), the effective angle of internal friction (δ), the apparent cohesion (C), the dilatancy angle (ψ), the grain-wall friction coefficient (μ), the effective grain-wall friction coefficient (μ_{ef}), and the apparent specific weight (γ_{ap}).

As the tests developed here were described in previous works in a general manner (Moya *et al.*, 2024, 2022; Moya-Ignacio *et al.*, 2024), only the specific information related to the tests conducted with wood pellets will be provided here.

2.1. Sample wetting

Sample wetting was possible with the help of the climatic chamber available at the laboratory. The parameters that must be fixed for the different tests conducted were temperature (ºC) and relative humidity (%).

The Standard (UNE-EN ISO 17225-1, 2022) considers five different categories of wood pellets depending on the moisture content, ranging from ≤ 5% up to ≤ 15%, expressing this moisture as a percentage by mass, as received, although a percentage lower than 10% (w.b.) is recommended (ENplus, 2023; UNE-EN ISO 17225-2, 2021). This parameter is important for reasons of storage safety and transport efficiency, since high moisture content (>15%) can cause spoilage during storage, while very low moisture content (<3%) can cause increased pellet crumbling (Tumuluru, 2016).

For the reasons outlined above, six different combinations of temperature and relative humidity were chosen for this study, so that the samples would reach six different levels of humidity. A minimum temperature of 20ºC was selected. For this temperature, four different relative humidity levels were chosen (35, 45, 55, and 65%). Additionally, the wood pellet sample was subjected to a temperature of 25ºC and a relative humidity of 50%. Finally, a temperature of 55ºC and 25% relative humidity was applied to the sample. The wood pellet samples were placed on a 20×40 cm stainless steel tray, without any covering. This ensured that all the pellets in the sample, which did not form a very high pile within the tray, could be exposed uniformly to the selected temperature and humidity conditions inside the climatic chamber. The tests could start once these temperature and humidity conditions had been maintained for at least 72 h in order to ensure that the sample was uniformly moist, as commented.

2.2. Oven drying

Oven drying was used in this research to determine the moisture content of the different samples tested. The drying temperature ranged between 105 and 110ºC. The tests were carried out in accordance with the standard (UNE-EN ISO 17892-1, 2015). An electronic balance accurate to 0.01 g was used to weigh the different samples every 24 h. The tests were completed once a constant weight was reached.

2.3. Direct shear test

The parameters determined with these tests were the angle of internal friction, effective angle of internal friction, apparent cohesion, and dilatancy angle. These tests adhered to the specifications established in part 10 of the standard (UNE-EN ISO 17892-10, 2018).

The main characteristics of this equipment, as well as the way in which the collected data is processed to obtain the corresponding results, have been described in previous studies (Moya *et al.*, 2024, 2022). In this research, a circular shear cell with a diameter of 10 cm was used, as shown in Fig. 1.

Normal stresses of 13, 25, 62, 125, 250, and 374 kPa were applied. A speed of 4 mm/min was selected for all tests performed, in accordance with that used in previous studies (Moya *et al.*, 2024; Moya-Ignacio *et al.*, 2024). Given that the total horizontal displacement allowed by the direct shear device is 20 mm, the test duration was 5 min,

Fig. 1. Circular shear cell 10 cm in diameter used in this research for the direct shear tests carried out with samples of wood pellets.

which helped to minimise moisture loss in the wood pellet samples. Three replications were carried out at each of the normal stresses applied to the sample.

Before the tests began, both half-boxes were aligned vertically by inserting through bolts. However, immediately before the test began, these bolts were removed to allow the lower half-box to move freely relative to the upper one as the carriage on which the two half-boxes were mounted was pushed at the speed selected to produce the direct shear through the wood pellet sample. Throughout the entire travel of the carriage, which was 20 mm, as previously commented, there was no control over the manner in which one half-box moved relative to the other, allowing the sample to deform freely.

According to Eurocode 1 Part 4 (UNE-EN-1991-4:2011/AC, 2013), the ratio between the sample size and the grain size should not be less than 40. Obviously, when testing wood pellets with the shear box used in this work, this ratio is far from that value. However, the interest of the results provided here outweighs the need to comply with this criterion, especially considering the limitations of the apparatus used, the impossibility of acquiring a larger device, and the direct shear tests carried out by other authors (Härtl and Ooi, 2011) which reduce the above limit to 5, similar to the ratio obtained in this research.

A modified shear box was used to determine the coefficient of grain-wall friction as well as the coefficient of effective grain-wall friction. As the shear box consists of two halves, the lower half was fitted with a sliding steel mould, whilst the upper half was filled with the wood pellet sample. This arrangement allowed the friction between the sliding steel surface and the wood pellet sample to be simulated during the test. In these tests, the applied normal stresses and the test velocity used were the same as those selected for the normal direct shear tests. Again, three replicates were carried out per wood pellet sample.

2.4. Tests for the determination of the apparent specific weight

An oedometer device was used for the determination of the apparent specific weight of the samples. The different oedometer tests were carried out using the three automatic oedometers available in the geotechnical laboratory in Plasencia.

The oedometric equipment was described in a previous work (Moya *et al.*, 2022). For this reason, only the specific characteristics of the tests conducted will be provided below. The tests were carried out in accordance with the standard (UNE-EN ISO 17892-5, 2017). Loading and unloading cycles were applied with normal stresses of 8, 16, 32, 64, 128, and 256 kPa. In this way, each loading step was doubled once primary consolidation was reached, while during the unloading cycle the applied load was reduced by half. Rapid oedometer tests were performed. In this way, each loading or unloading step could take place once primary consolidation did not reach 0.1 mm for 3 h, which reduced the duration of the tests and thus minimised moisture loss from the sample.

In this test, an oedometric cell of known volume was used, so that the sample of wood pellets was weighed before being placed inside the cell, thus determining its initial apparent specific weight. In this way, as the test progresses, the height of the sample can be determined as it is compressed or decompressed, depending on whether the loading or unloading cycle is being performed, thus determining its apparent specific weight. A more detailed explanation can be found in a previous work (Moya *et al.*, 2024).

2.5. Statistical analysis

A statistical analysis was carried out to determine possible relationships between moisture content and the selected parameters. For each level of normal stress, Pearson's correlation coefficient and the corresponding p-value from simple linear regression models were calculated to assess the relationship between moisture content and the parameter of interest. Furthermore, linear regression models including an interaction term between moisture content and normal stress were fitted to evaluate their combined effect on shear stress and apparent specific weight. Statistical significance was assessed at the 95% confidence level. Statistical analyses were performed using Microsoft Excel 365, IBM SPSS Statistic v. 22 and R v. 4.6.0. Partial dependence plots were generated with the pdp package.

3. RESULTS

3.1. Moisture content

The wood pellet samples were placed inside the climatic chamber available in the laboratory and subjected to different combinations of temperature and relative humidity. Specifically, the different combinations of temperature and relative humidity selected, and their corresponding moisture contents expressed on a dry basis (d.b.) and obtained from weighing carried out after oven drying at a temperature ranging between 105 and 110ºC, are shown in Table 1.

Table 1. Moisture content, expressed as dry basis (d.b.), of the wood pellet samples from the different combinations of temperature and relative humidity

Climatic chamber conditions		Moisture content (d.b.) (%)
Temperature (°C)	Relative humidity (%)	
20	35	6.7
20	45	8.4
20	55	10.0
20	65	12.0
25	50	8.4
55	25	5.0

The range of values shown above varies between 5.0 and 12.0%, which is within the recommended range (ENplus, 2023; UNE-EN ISO 17225-2, 2021) and that selected in other studies (Masche *et al.*, 2023; Molenda and Horabik, 2005; Wu *et al.*, 2011).

It should be noted that not all of these combinations could be applied in every test carried out in this study. Therefore, for each type of the test conducted, the corresponding moisture contents listed in the table above will be indicated. In addition, the results obtained from the oedometer tests under ambient conditions have been included. These tests were already carried out in previous studies (Moya *et al.*, 2022) and did not require the use of a climatic chamber, as these results had never been published before, and they refer to a moisture content of 6.4%. Hence, it was not necessary to carry out further tests by preparing the sample in the climatic chamber at a temperature of 20°C and a relative humidity of 35% to obtain a moisture content of 6.7%, as this moisture content is very similar to that achieved under ambient conditions.

3.2. Direct shear tests

3.2.1. Angle of internal friction, effective angle of internal friction, and apparent cohesion

Based on the direct shear tests performed, stress-strain curves were obtained for the wood pellets at different normal stresses applied. Figure 2a, b show the curves obtained with moisture contents of 5.0 and 12.0%, respectively. These graphs show the mean value obtained for the shear stress at each horizontal displacement value and its corresponding standard deviation. The latter is represented by vertical bars.

The Fig. 2 demonstrate how the material's behaviour varies, depending on its moisture content. Thus, for a moisture content of 5.0%, similar curves were obtained for the lower normal stresses applied (13 and 25 kPa), whilst the

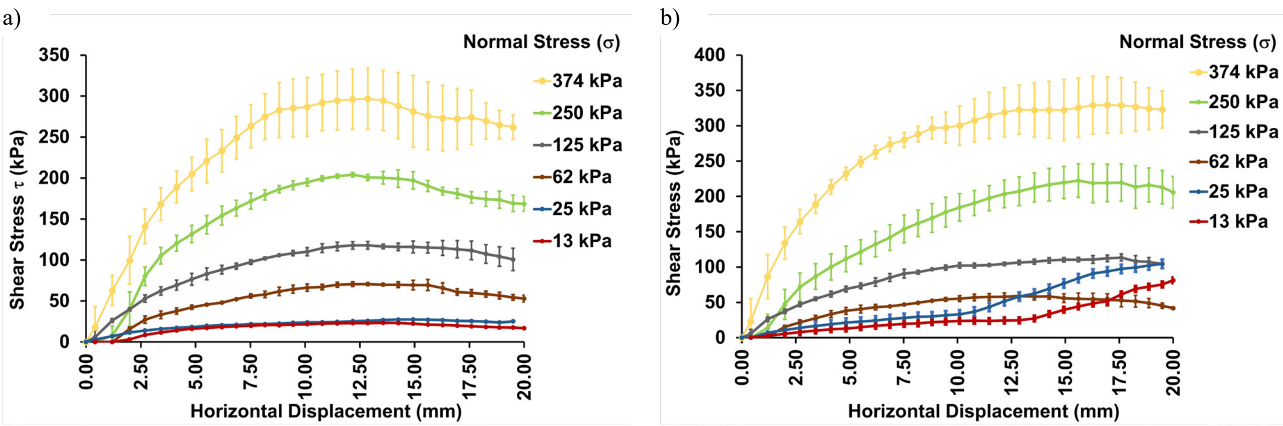

Fig. 2. Stress-strain curves and their corresponding standard deviation for wood pellets depending on the normal stress applied in the different direct shear tests carried out at a moisture content of: a) 5.0, and b) 12% d.b.

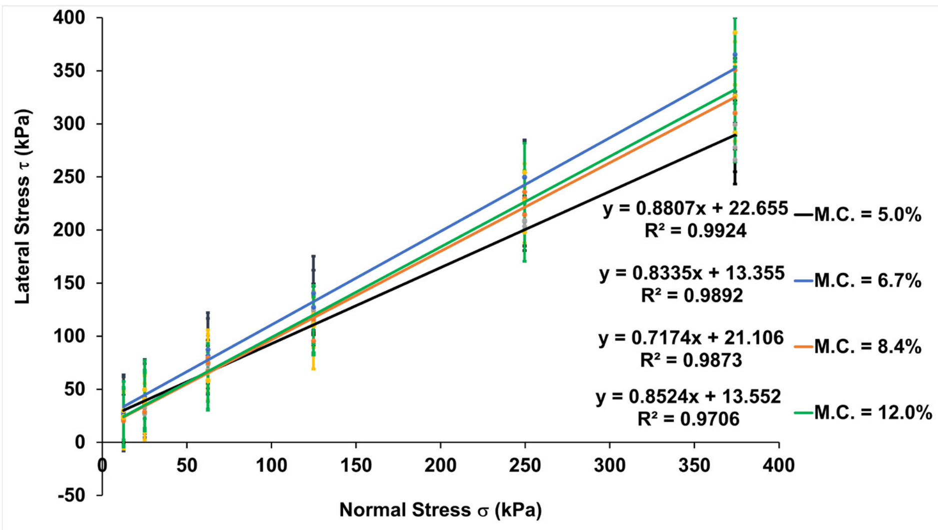

Fig. 3. Regression lines obtained from the Mohr-Coulomb strength envelopes as a function of the normal stress applied and for the different moisture contents tested (M.C. – moisture content).

curves obtained with the higher normal stresses differed markedly, depending on the stress state reached under the different normal stresses. For the intermediate moisture contents applied (8.4 and 6.7%, respectively), the graphs obtained were similar to that shown in Fig. 2a, with the curves corresponding to the different shear stresses applied being quite far apart from one another. However, for a moisture content of 12.0%, the curves obtained at normal pressures of 13 and 25 kPa showed a similar trend. Thus, both curves lay below that corresponding to a normal pressure of 62 kPa. Nevertheless, at high values of horizontal displacement an increase in shear stress was observed, reaching values even higher than those obtained with the normal stress, which was unexpected given that the stress state was lower.

When comparing the results obtained at moisture contents of 5.0 and 12.0%, it can be seen that the maximum shear stress (329.47 kPa) was achieved at a normal stress of 374 kPa and a moisture content of 12.0%, whereas the maximum value achieved with the same normal stress and a moisture content of 5.0% was 296.84 kPa. Therefore, the maximum shear stress was 11% higher with the highest moisture content applied. Conversely, when analysing the maximum value reached in the curves that provided the lowest values of the shear stress with these moisture contents, the lowest value (23.33 kPa) was achieved with a moisture content of 5.0% and a normal stress of 13 kPa, whilst this value was 58.94 kPa with a normal stress of 62 kPa and a moisture content of 12.0%. Therefore, the minimum shear stress was 253% lower at 5% moisture content compared to the minimum value achieved at the highest moisture content (12.0%).

Using the Mohr-Coulomb strength envelopes, regression lines were obtained for the different moisture contents and normal stresses applied to the wood pellet samples. These lines are shown in Fig. 3.

Table 2. Mean values and standard error of the angle of internal friction, effective angle of internal friction and the apparent cohesion of the wood pellet sample for the four moisture contents assayed

Moisture content (%) (d.b.)	Angle of internal friction (φ, °)	Effective angle of internal friction (δ, °)	Apparent cohesion (C, kPa)
5.0	35.7 ± 0.8	38.6 ± 0.8	21.11 ± 3.92
6.7	41.4 ± 0.8	44.0 ± 0.9	22.66 ± 4.70
8.4	39.8 ± 0.7	41.4 ± 0.6	13.36 ± 4.18
12.0	40.4 ± 1.2	42.1 ± 0.9	13.55 ± 7.14

The previous figure shows the mathematical expression corresponding to each line obtained for each of the moisture contents applied in each case. These expressions made it possible to determine the mean values and standard error of the angle of internal friction, effective angle of internal friction, and apparent cohesion. These values are shown in Table 2.

Table 2 shows that the highest value for the angle of internal friction (41.4º) was obtained at a moisture content of 6.7%, whilst the lowest value for this parameter (35.7º) was recorded at a moisture content of 5.0%. Therefore, the maximum value achieved was 16% higher than the minimum obtained. However, in the case of the effective angle of internal friction, this difference was reduced to 14% between the maximum (44.0º) and minimum (38.6º) values recorded at moisture contents of 6.7 and 5.0%, respectively. Finally, when considering the ratio between the effective angle of internal friction and the angle of internal friction, this relationship ranged from 4.0% for a moisture content of 8.4 to 8.1% for a moisture content of 5.0%.

When analysing the relationship between the moisture content of the sample and the values obtained for the angle of internal friction, no general trend could be identified. This was because this value decreased at a moisture content of 8.4% compared with that recorded at a moisture content of 6.7%, and furthermore, the value obtained at the maximum moisture content applied (12.0%) did not exceed that achieved at 6.7%. As expected, the same conclusion was reached in the case of the effective angle of internal friction.

As regards the values obtained for apparent cohesion, it should be noted that these were not particularly high for moisture contents of 8.4 and 12.0%, whilst they were slightly higher for moisture contents of 5.0 and 6.7%. For this reason, no general trend could be identified for this parameter as the moisture content increased. The highest value for this parameter (22.66 kPa) was obtained at a moisture content of 6.7%. This value was 69.6% higher than the minimum (13.36 kPa), which was achieved at a moisture content of 8.4%.

Given that both the angle of internal friction and the apparent cohesion are determined from the regression lines obtained by plotting shear stress against normal stress, direct statistical comparisons were not considered appropriate for these parameters. Therefore, an additional analysis was performed on the original measurements. The results revealed a significant interaction between normal stress and moisture content on shear stress ($p = 0.011$), as shown in Fig. 4.

The results obtained for these parameters were analysed at low (13, 25 and 62 kPa) and high (125, 250 and 374 kPa) normal pressures. The regression lines of the Mohr-Coulomb strength envelopes are plotted in Fig. 5a,b,c showing the results obtained for moisture contents of 6.7, 12.0, and 8.4%, respectively. In these figures, M.C. means moisture content.

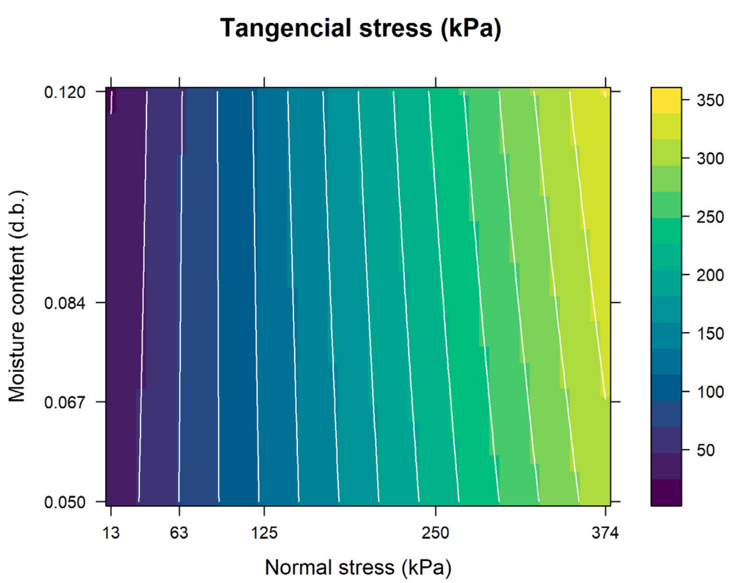

Fig. 4. Influence of moisture content and normal stress on shear stress, based on the fitted interaction model.

a) b) c)

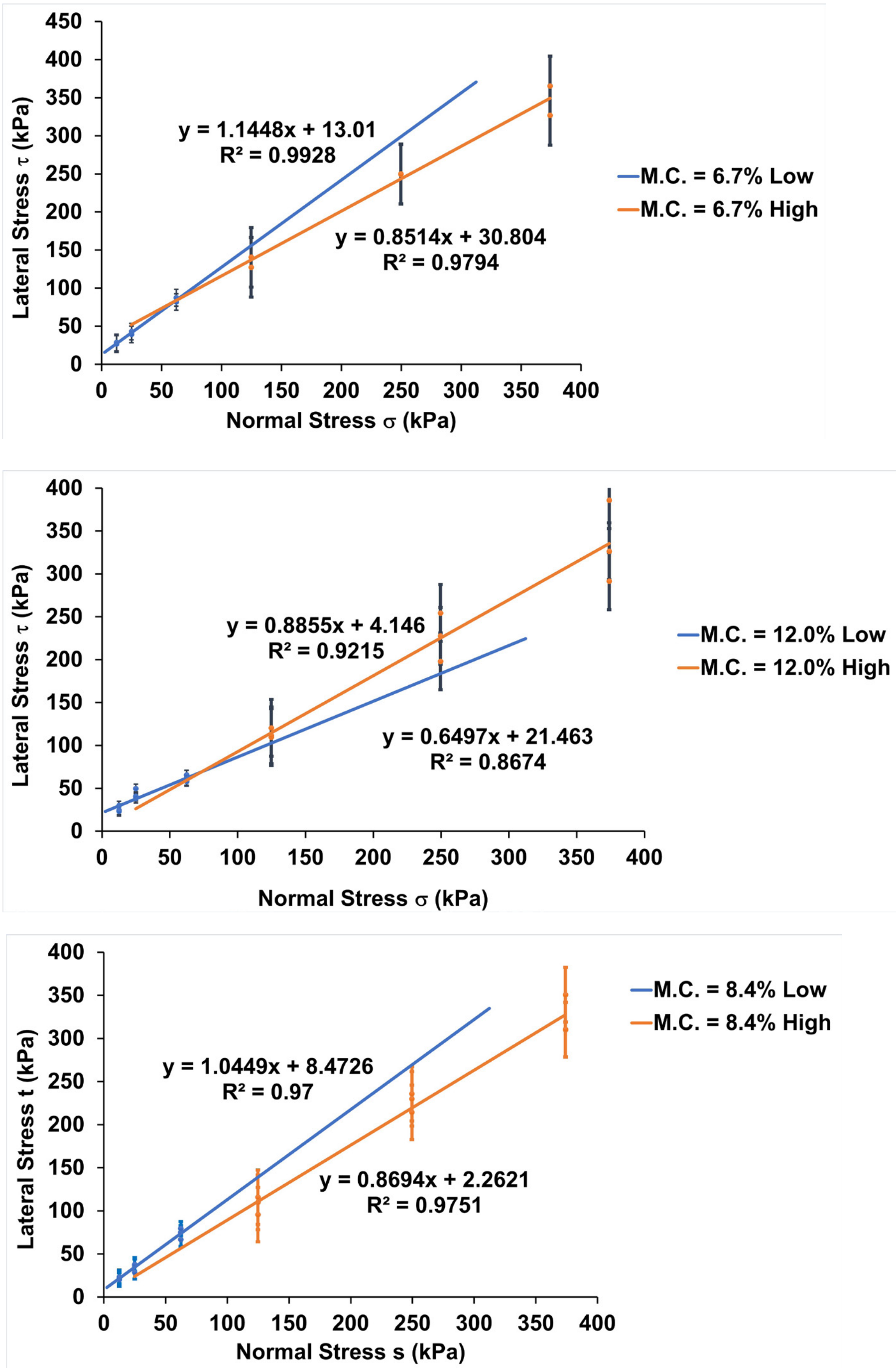

Fig. 5. Regression lines of the Mohr-Coulomb strength envelopes at low (13, 25 and 62 kPa) and high (125, 250 and 374 kPa) normal pressures at a moisture content of: a) 6.7, b) 12, and c) 8.4%.

These figures show three different behaviours of the material tested at the four moisture contents applied. The first (Fig. 5a) shows that the slope of the regression line obtained at a moisture content of 6.7% and a low normal stress is greater than that obtained at a high normal stress. Furthermore, both curves intersect at a normal stress of around 62 kPa. However, in the second figure (Fig. 5b), the slope of the regression line obtained with a moisture content of 12.0% and high normal stress is greater than that obtained with low normal stress. In this case, both curves intersect again at a normal stress slightly greater than 62 kPa. Finally, in the last figure (Fig. 5c), the slope corresponding to the regression line with a moisture content of 8.4% and low normal stress is greater than that obtained with high moisture content, but in this case they do not intersect. Finally, although not shown in the previous figures, regression lines obtained with a moisture content of 5.0% were similar to those illustrated in Fig. 5a for a moisture content of 6.7%. In all cases, given that the slopes of the regression lines differed depending on the normal stress

Table 3. Mean values and standard error of the angle of internal friction, effective angle of internal friction and apparent cohesion of the wood pellet sample for the four moisture contents assayed, at low (13, 25 and 62 kPa) and high (125, 250 and 374 kPa) normal stresses

Moisture content (%) (d.b.)	Angle of internal friction (φ, °)		Effective angle of internal friction (δ, °)		Apparent cohesion (C, kPa)	
	Low normal stress	High normal stress	Low normal stress	High normal stress	Low normal stress	High normal stress
5.0	46.1 ± 2.2	32.6 ± 1.4	50.1 ± 1.3	38.3 ± 0.9	7.42 ± 3.13	43.34 ± 9.00
6.7	48.9 ± 1.2	40.4 ± 2.0	54.8 ± 1.3	43.8 ± 0.8	13.01 ± 1.92	30.80 ± 16.63
8.4	46.3 ± 1.9	41.0 ± 1.7	50.4 ± 1.1	41.2 ± 0.6	8.47 ± 2.74	2.26 ± 14.16
12.0	33.0 ± 3.9	41.5 ± 3.1	47.9 ± 2.9	42.0 ± 1.1	21.46 ± 3.79	4.15 ± 26.32

range considered (low or high), both the internal friction angles and the corresponding apparent cohesions were also different. From the various regression lines obtained, the mean values and standard error for the angle of internal friction, effective angle of internal friction, and apparent cohesion were calculated for each of the moisture contents applied at low and high normal stresses. Table 3 shows the results obtained for these parameters.

The preceding table shows that the values of the angle of internal friction obtained were higher at low normal stresses than at high normal stresses, except when a moisture content of 12.0% was applied. The highest value for this parameter (48.9º) was achieved at a moisture content of 6.7% under low normal stresses, whilst the lowest value (32.6º) was obtained at a moisture content of 5.0% and at high normal stresses. Therefore, the maximum value was 50% higher than the minimum. When analysing the values obtained under low normal stresses, the highest value (48.9º) achieved at a moisture content of 6.7 was 48% higher than the minimum (33º) achieved at a moisture content of 12.0%. In the case of high normal stresses, this difference was 27% between the highest value obtained (41.5º) when applying a moisture content of 12.0% and the lowest value (32.6º) at a moisture content of 5.0%. Finally, when considering only the values obtained at high normal stresses, it was observed that the higher the moisture content applied, the higher the values obtained for the angle of internal friction. However, when a similar analysis was carried out using the values obtained at low normal stresses, the maximum value was reached at a moisture content of 6.7% and, from that point onwards, decreased as the moisture content increased.

As regards the values for the effective angle of internal friction, those obtained under low normal stresses were higher than those obtained under high normal stresses for all four moisture contents analysed. The highest value (54.8°), obtained with low normal stresses and a moisture content of 6.7%, was 43.1% higher than the minimum (38.3°), which was recorded with high normal stresses and a moisture content of 5.0%. When only low normal stresses were analysed, the maximum value (54.8°) was 14.4% higher than the minimum (47.9°), with these values being reached at moisture contents of 8.4 and 12.0%, respectively. Furthermore, the same difference (14.4%) was recorded between the maximum (43.8°) and minimum (38.3°) values when only high normal stresses were analysed, with these values being attained at moisture contents of 6.7 and 5.0%, respectively. Finally, when analysing the relationship between moisture content and the values of the effective angle of internal friction, considering only low normal stresses on the one hand and subsequently high normal stresses on the other, no correlation could be detected in either case.

With respect to apparent cohesion, the maximum and minimum values were observed in the high normal stress range. Thus, the maximum value (43.34 kPa) was recorded at a moisture content of 5.0%, whilst the minimum (2.26 kPa) was recorded at a moisture content of 8.4%. Consequently, the maximum value was approximately nineteen times greater than the minimum. When analysing the low normal stress range, the maximum value (21.46 kPa) was reached at a moisture content of 12.0%, whilst the minimum (7.42 kPa) was reached at a moisture content of 5.0%. In this case, the difference between these values was 289%, *i.e.* the maximum value was approximately three times greater than the minimum. In both the low and high normal stress ranges, no general trend was observed, as the increase in moisture content values did not cause an increase or decrease in the apparent cohesion values.

Graphs similar to that shown in Fig. 4 were obtained when analysing the relationship between shear stress and normal stress and moisture content at low and high normal stresses. In these cases, the interaction term remained statistically significant, with p-values of < 0.001 and 0.031, respectively.

3.2.2. Dilatancy angle

As explained in the Materials and Methods section, direct shear tests were used to determine the dilatancy angle. This parameter was calculated from the values of vertical strain

(ε_v) and horizontal displacement (ε_H) recorded during the direct shear test. Various graphs were obtained showing the deformation curves and the corresponding error bars (standard deviation) for each of the moisture contents applied to the wood pellet samples at different normal stresses. The most representative of these are shown in Fig. 6a, b.

These figures show the different trends observed as the direct shear test is carried out. These curves correspond to the average values obtained from the three replications performed for each normal stress applied. Figure 6a, obtained at a moisture content of 6.7%, represents the most logical a priori distribution of the different curves as a function of

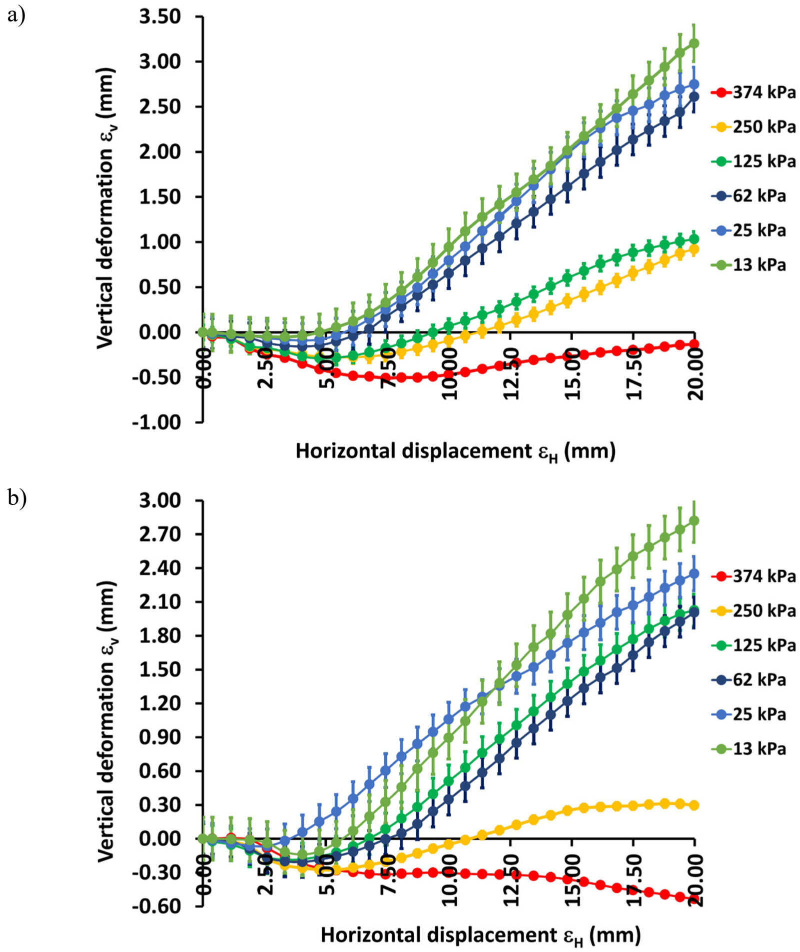

Fig. 6. Deformation curves and error bars obtained for wood pellet samples at a moisture content of: a) 6.7 and b) 5.0%.

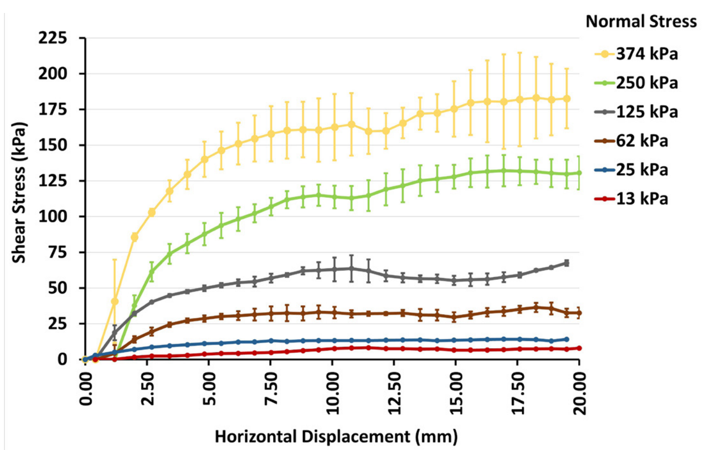

Fig. 7. Stress-strain curves and their corresponding standard deviation for wood pellets depending on the normal stress applied in the different direct shear tests carried out using a modified shear cell at a moisture content of 8.4% d.b.

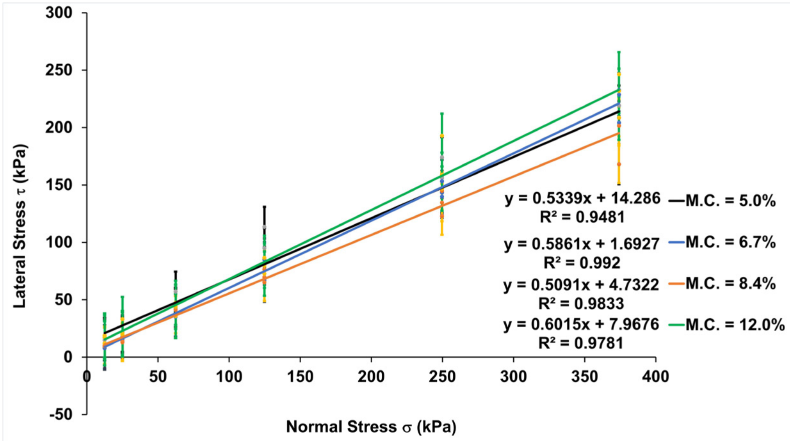

Fig. 8. Regression lines obtained from the Mohr-Coulomb strength envelopes as a function of the normal stress applied and for the different moisture contents tested in the direct shear tests carried out using a modified shear cell (M.C. – moisture content).

the normal stress applied. In this case, the greater the normal stress, the smaller the expansion of the sample. In the tests carried out at a moisture content of 8.4%, the behaviour of the sample was similar to that described here. However, this trend was not observed in all cases, as shown in Fig. 6b for a moisture content of 5.0%. In this case, the curve corresponding to a normal stress of 125 kPa lay above that obtained at a normal stress of 62 kPa. Furthermore, for values below approximately 11 mm of horizontal displacement, the curve corresponding to a normal stress of 25 kPa lay above that of 13 kPa. For a moisture content of 12.0%, the result was similar to that shown in Fig. 12. In this case, the average vertical deformation obtained when applying a normal stress of 62 kPa was greater than that obtained at a normal stress of 25 kPa when the horizontal displacement exceeded 15 mm. Table 4 lists the mean values and standard deviation obtained for the dilatancy angle, depending on the normal stress and moisture content applied.

The table above shows that the maximum value (35.6º) was reached when a moisture content of 12.0% and a normal stress of 13 kPa were applied, whilst the minimum (1.1º) was recorded at the same moisture content (12.0%) but under a normal stress of 250 kPa. As a general trend, the dilatancy angle decreased as the normal stress increased, although there were some exceptions, such as those recorded when a moisture content of 5.0% and a normal stress of 62 kPa were applied, as well as that observed with a moisture content of 6.7% and a normal stress of 25 kPa and that observed with a moisture content of 12.0% and a normal stress of 250 kPa.

When analysing the influence of moisture content on dilatancy angle values, a significant inverse correlation was observed between the dilatancy angle and moisture content at a normal stress of 250 kPa ($r_{pearson}$ = -0.77, p = 0.005), as well as a significant positive correlation at a normal stress of 374 kPa ($r_{pearson}$ = 0.62, p = 0.041). However, no significant interaction was observed between normal stress and moisture content on the dilatancy angle (p = 0.582). It can therefore be concluded that no general trend was observed in this study, as the association between the dilatancy angle and moisture content varied across the normal stress levels examined. An irregular trend was observed in this regard

Table 4. Mean values and standard deviation of the dilatancy angle for wood pellets at each normal stress and moisture content applied

Normal stress (kPa)	Dilatancy angle (ψ, º)				Linear regression model	
	Moisture content (d.b.)					
	5.0%	6.7%	8.4%	12.0%	$r_{pearson}$	p-value
13	35.3 ± 0.8	34.3 ± 4.6	32.5 ± 5.3	35.6 ± 2.5	0.04	0.897
25	28.2 ± 5.3	34.9 ± 2.3	26.8 ± 5.9	28.5 ± 3.7	-0.12	0.727
62	28.5 ± 5.7	29.9 ± 2.4	21.8 ± 1.9	23.2 ± 2.8	-0.54	0.085
125	27.8 ± 4.4	18.2 ± 0.8	17.3 ± 2.0	18.7 ± 4.4	-0.56	0.072
250	11.7 ± 1.7	16.7 ± 2.1	5.0 ± 5.1	1.1 ± 1.8	-0.77	0.005
374	3.4 ± 3.5	7.7 ± 0.8	4.9 ± 2.9	10.1 ± 3.4	0.62	0.041

Table 5. Mean values and standard error of the grain-wall friction coefficient, coefficient of effective grain-wall friction and their corresponding angles, of the wood pellet sample for the four moisture contents assayed using a slippery steel mould

Moisture content (%) (d.b.)	Coefficient of grain-wall friction (μ)	Grain-wall friction angle (ϕ_w, °)	Coefficient of effective grain-wall friction (μ_{ef})	Effective grain-wall friction angle (ϕ_{wef}, °)
5.0	0.53 ± 0.03	28.1 ± 1.4	0.59 ± 0.02	30.5± 1.0
6.7	0.59 ± 0.01	30.4 ± 0.6	0.59 ± 0.01	30.6± 0.4
8.4	0.51 ± 0.02	27.0 ± 0.8	0.53 ± 0.01	27.8± 0.5
12.0	0.60 ± 0.02	31.0 ± 0.9	0.63 ± 0.02	32.3± 0.7

and, consequently, it was not possible to link an increase or decrease in the values of this parameter to an increase or decrease in the moisture content applied.

Finally, when considering the difference between the maximum and minimum values recorded for this parameter at each moisture content applied, it should be noted that the greatest percentage drop (96.9%) was recorded at a moisture content of 12.0%, as the maximum value at this moisture content was 35.6º and the minimum 1.1º. Meanwhile, the second largest percentage drop was recorded at a moisture content of 5.0% (90.1%), whilst the drop observed at a moisture content of 8.4% was 84.9% and the lowest (77.7%) was recorded at a moisture content of 6.7%, with a maximum value of 34.9º and a minimum of 7.8º.

3.2.3. Grain-wall friction

The grain-wall friction coefficient, the corresponding grain-wall friction angle, as well as the coefficient of effective grain-wall friction and the corresponding effective grain-wall friction angle, were determined from direct shear tests carried out using a modified shear cell, as explained in the 'Materials and Methods' section. The shape of the stress-strain curves obtained by applying the different moisture contents selected in this study presented a trend similar to that shown in Fig. 7 for a moisture content of 8.4%. This figure shows the mean value of the shear stress at each horizontal displacement value and its corresponding standard deviation, represented by vertical bars.

As can be seen in the figure above, in all cases the curves corresponding to each of the shear stresses applied were quite far apart from each other. In addition, for the four moisture contents applied in the direct shear tests, the higher the normal stress applied, the higher the shear stress. Therefore, the curve that provided the highest values of the shear stress corresponded to that obtained at a normal stress of 374 kPa, whilst the curve that provided the lowest values of this parameter was obtained at a normal stress of 13 kPa.

When comparing the maximum values obtained for the shear stress at the different moisture contents applied, the highest value (226.88 kPa) was achieved at a moisture content of 12.0%, whilst the minimum (183.17 kPa) was provided at a moisture content of 8.4%. Therefore, the difference between these highest and lowest values was 23.9%. Conversely, the maximum values within the curves that provided the minimum values of the shear stress (as commented above, in all cases it happened when a normal stress of 13 kPa was applied), were analysed as well. The maximum value (15.22 kPa) was achieved at a moisture content of 12.0%, whilst the minimum (8.01 kPa) was recorded when a moisture content of 6.7% was applied. Therefore, the highest value was 90% greater than the minimum in this case.

Figure 8 shows the regression lines obtained from the corresponding Mohr-Coulomb strength envelopes:

As with the results provided for the standard direct shear tests, the previous figure shows the mathematical expressions used to represent each curve obtained for each of the moisture contents applied. Based on these expressions, the mean values and standard error of the grain-wall friction coefficient, the coefficient of effective grain-wall friction, and their corresponding angles were calculated, as shown in Table 5.

From this table, it can be seen that the highest value for the grain-wall friction coefficient (0.60) was recorded at a moisture content of 12.0%, whilst the lowest value for this parameter (0.51) was obtained at a moisture content of 8.4%. Therefore, the highest value was 18% greater than the minimum. In addition, no general trend could be observed between the values of the grain-to-wall friction coefficient and the moisture content of the sample. In this case, the p-value obtained was 0.136, revealing that the combined influence of normal stress and moisture content on shear stress was not statistically significant. However, in the case of the coefficient of effective gran-wall friction, the maximum value (0.63), obtained at a moisture content of 12.0%, was 18.9% greater than the minimum (0.53) obtained at a moisture content of 8.4%. The values of both coefficients were also expressed in degrees, so that they can be analysed later by comparing them with those reported in the literature.

The most significant results obtained when considering low (13, 25, and 62 kPa) and high (125, 250, and 374 kPa) normal stresses at the different moisture contents applied are shown below. The regression lines of the Mohr-Coulomb strength envelopes for moisture contents of 8.4 and 12.0% are plotted in Fig. 9a and 9b, respectively.

a)

b)

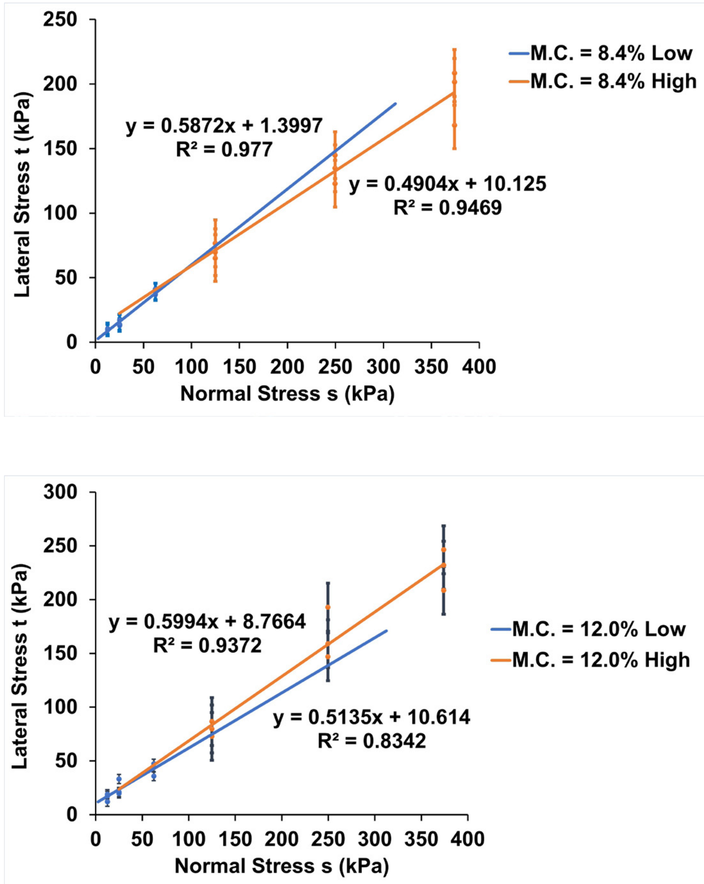

Fig. 9. Regression lines obtained from the Mohr-Coulomb strength envelopes at low (13, 25 and 62 kPa) and high (125, 250 and 374 kPa) normal stresses at a moisture content of: a) 8.4 and b) 12.0% using a modified shear box (M.C. – moisture content).

The preceding figures show two distinct behaviours of the material under analysis, depending on the different moisture contents applied to the wood pellet samples in this study. Thus, in Fig. 9a, for a moisture content of 8.4%, the slope of the regression line obtained with low normal stresses is greater than that obtained with high normal stresses. Furthermore, both lines intersect at around 90 kPa. The opposite case is illustrated in Fig. 9b, where the slope of the regression line obtained with high normal stresses is greater than that corresponding to low normal stresses. In this case, both lines intersect at a very low normal stress value, around 20 kPa. Meanwhile, the result obtained with a moisture content of 5.0% is similar to that shown in Fig. 9a, although in this case the point of intersection occurs at a higher normal stress, around 160 kPa, whereas the graph obtained with a moisture content of 6.7% is quite similar to that shown in Fig. 9b, but both lines intersect at a lower normal stress, very close to 0 kPa.

Table 6 lists the mean values and standard error obtained for the grain-wall friction coefficient, the coefficient of effective grain-wall friction, and their corresponding angles expressed in degrees at low and high normal stresses and for the various moisture contents applied to the wood pellet samples.

In this table, the values obtained for the grain-wall friction coefficient ranged from 0.42 to 0.69. The former was achieved under high normal stresses at a moisture content of 5.0%, whilst the latter was recorded under low normal stresses at the same moisture content (5.0%). Therefore, the maximum value was 64% greater than the minimum. When analysing the difference between the maximum and minimum values obtained with high normal stresses, the maximum value (0.60 at a moisture content of 12.0%) was 43% higher than the minimum (0.42 at a moisture content of 5.0%), whereas this difference was 35% between the maximum (0.69 at 5.0% moisture content) and the minimum (0.51 at 12.0% moisture content) when only low normal stresses were considered. The statistical analysis showed that p-values associated with the interaction term were 0.170 at low normal stresses and 0.071 at high normal stresses. Therefore, for neither high nor low normal stresses was there any general trend that would allow a correlation to be detected between the grain-wall friction value and the moisture content applied.

As regards the values of the coefficient of effective grain-wall friction, the maximum value (0.77) was achieved at a moisture content of 5.0% and low normal stresses, whilst the minimum (0.52) was recorded at a moisture content of

Table 6. Mean values and standard error of the grain-wall friction coefficient (μ), the coefficient of effective grain-wall friction (μ_{ef}), and their corresponding values in degrees (ϕ_w and ϕ_{wef}, respectively) for the four moisture contents assayed at low (13, 25, 62 kPa) and high (125, 250 and 374 kPa) using a slippery steel mould

Moisture content (%) (d.b.)		Grain-wall friction				Effective grain-wall friction			
		Low normal stress		High normal stress		Low normal stress		High normal stress	
		μ	ϕ_w (°)	μ	ϕ_w (°)	μ_{ef}	ϕ_{wef} (°)	μ_{ef}	ϕ_{wef} (°)
5.0	Mean	0.69	34.7	0.42	22.6	0.77	37.7	0.58	30.3
	St. dev.	0.06	3.2	0.06	3.2	0.05	1.6	0.03	1.4
6.7	Mean	0.53	28.1	0.58	30.0	0.60	30.8	0.59	30.6
	St. dev.	0.04	1.7	0.03	1.5	0.02	1.0	0.01	0.5
8.4	Mean	0.59	30.4	0.49	26.1	0.62	31.7	0.52	27.7
	St. dev.	0.03	1.5	0.04	2.0	0.02	0.8	0.02	0.7
12.0	Mean	0.51	27.2	0.60	30.9	0.74	36.5	0.63	32.2
	St. dev.	0.07	3.9	0.04	2.5	0.07	2.5	0.02	0.9

8.4% and high normal stresses. Therefore, the former was 48.1% higher than the latter. Furthermore, the analysis of the values obtained under high normal stresses showed that the difference between the maximum value (0.63), obtained at a moisture content of 12.0%, and the minimum (0.52), obtained at a moisture content of 8.4%, was 21.2%. In the case of the low normal stresses, this difference was 28.3% between the maximum (0.77) and minimum (0.60) values obtained with moisture contents of 5.0 and 6.7%, respectively. Once again, no general trend could be detected for either high or low normal stresses that correlated the values of the coefficient of effective grain-wall friction with the moisture content.

3.2.4. Dilatancy angle using a modified shear cell

Direct shear tests carried out using the modified shear cell also made it possible to determine the dilatancy angle resulting from the interaction between the wood pellet particles and the slippery steel mould used. The deformation curves obtained in this test mode showed two different trends. The first corresponded to a situation in which, under most of the normal stresses applied, a large proportion of the various curves lay on the positive y-axis, exhibiting a positive dilation. This behaviour was observed at moisture contents of 5.0 and 12.0%. Conversely, when the two remaining moisture contents were applied, the corresponding curves all lay below the x-axis although for most of the normal stresses applied the specimen also exhibited positive dilation. Figure 10a, b illustrate these behaviours for moisture contents of 12.0 and 6.7%, respectively.

In both Fig. 10a, b, the curves corresponding to normal stresses of 250 and 374 kPa lie below the x-axis; however, in the latter, the curve obtained for a normal stress of 250 kPa lies well below that obtained at 374 kPa, which was unexpected. Furthermore, in both cases, the curves obtained at a normal stress of 25 kPa were situated above that corresponding to 13 kPa at high values of horizontal displacement (around 17-18 mm).

From these figures, the dilatancy angle values were obtained. Table 7 lists the mean values and standard deviation of this parameter as a function of the normal stresses and moisture contents applied in each case.

This table shows that the dilatancy angle values obtained in the direct shear tests using a modified shear box ranged from 22.3 to 0.6º. The former was obtained at a moisture content of 12.0% and a normal stress of 13 kPa, whilst the latter was achieved when moisture contents of 8.4 and 12.0% were applied under a normal stress of 374 kPa. In most cases, the higher the normal stress applied, the lower the dilatancy angle obtained for all moisture contents tested, although there were some exceptions, such as those observed at a normal stress of 25 kPa and moisture contents of 5.0 and 6.7%, as well as those recorded at a moisture content of 8.4% at normal stresses of 25 and 125 kPa, or that recorded at a normal stress of 25 kPa for a moisture content of 12.0%.

According to what was observed in standard direct shear tests, the p-value obtained for the interaction term was 0.348, indicating that no significant interaction was observed between normal stress and moisture content on the dilatancy angle when the shear box was modified. Likewise, no significant correlations were observed between the moisture content and the dilatancy angle at any normal stress level.

a)

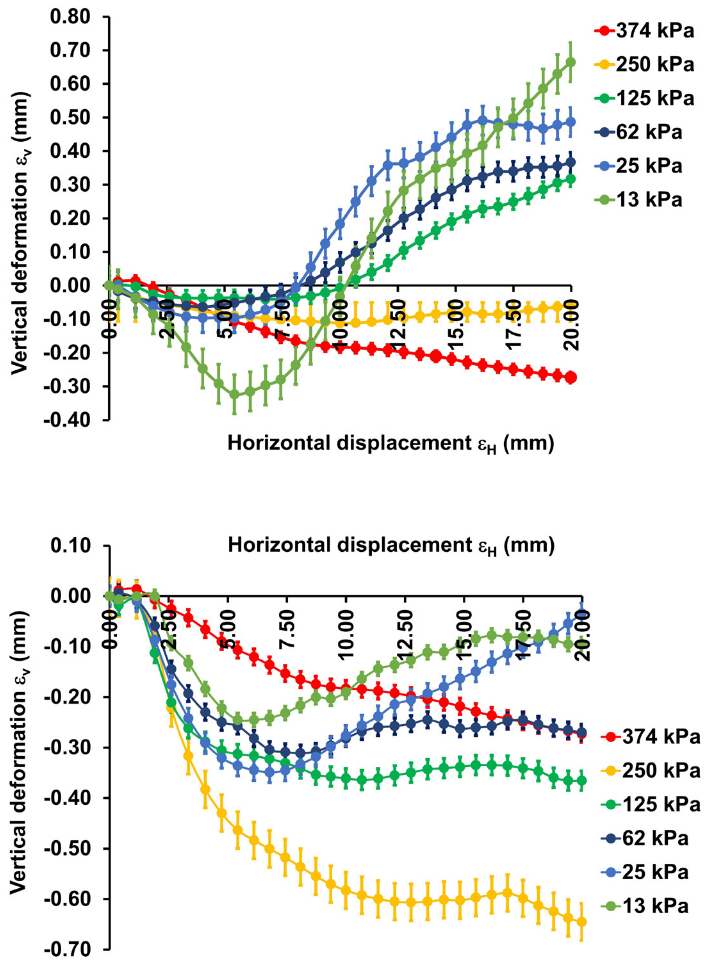

Fig. 10. Deformation curves and error bars obtained for wood pellets from direct shear tests using a modified shear box and at a moisture content of: a) 12.0 and b) 6.7%.

When analysing the differences between the maximum and minimum values obtained for this parameter at each of the moisture contents tested, it was observed that the greatest percentage drop (97.3%) was recorded at a moisture content of 12.0%, followed by that obtained at a moisture content of 8.4% (95.0%), whilst this percentage decrease was 90.2% at a moisture content of 6.7% and the lowest (82.1%) was recorded at a moisture content of 6.7%.

Finally, when comparing the maximum values obtained for this parameter at each of the moisture contents analysed with the maximum values recorded in standard direct shear tests for the same moisture contents, it was found that the latter were higher than the former. These differences ranged between 59.6%, for a moisture content of 12.0 to 401% for a moisture content of 6.7%.

3.3. Oedometer tests

Oedometer tests were carried out to analyse the influence of moisture content and applied normal stress on the apparent specific weight of the wood pellet samples. To this end, the apparent specific weight was first plotted on the ordinate axis, whilst the applied normal stress was plotted on the abscissa axis. Figure 11 shows the various curves obtained, which illustrate the variation of the apparent specific weight as a function of the applied normal stress for the moisture contents analysed.

The table above shows that, as expected, the higher the normal stress applied, the greater the apparent specific weight. Furthermore, the general trend observed was that the higher the moisture content of the wood pellet samples, the greater the apparent specific weight. The only exception to this trend was the curve obtained for a moisture content of 6.4%, which exceeded that corresponding to a moisture content of 8.4% when a normal stress of 256 kPa was applied during the loading cycle and throughout the unloading cycle.

Similarly, the apparent specific weight can be plotted against moisture content for different applied normal stresses. Figure 12 shows the relationship between these two parameters. In this case, only the loading cycle was taken into account.

Table 7. Mean values and standard deviation of the dilatancy angle at each normal stress and moisture content applied in the direct shear tests conducted using a modified shear cell

Normal stress (kPa)	Dilatancy angle (ψ, °)				Linear regression model	
	Moisture content (d.b.)					
	5.0%	6.7%	8.4%	12.0%	$r_{pearson}$	p-value
13	20.1 ± 3.3	8.4 ± 8.8	12.0 ± 4.7	22.3 ± 1.4	0.29	0.365
25	20.4 ± 2.5	8.7 ± 0.1	4.3 ± 2.4	21.2 ± 2.2	0.16	0.619
62	13.2 ± 6.2	4.4 ± 0.8	6.9 ± 3.0	9.9 ± 2.1	-0.08	0.800
125	11.1 ± 4.5	4.1 ± 2.4	1.3 ± 1.5	10.7 ± 1.0	0.08	0.816
250	3.1 ± 1.8	1.7 ± 1.6	2.4 ± 1.6	3.7 ± 0.6	0.26	0.419
374	2.0 ± 1.6	1.5 ± 1.1	0.6 ± 0.9	0.6 ± 0.4	-0.49	0.107

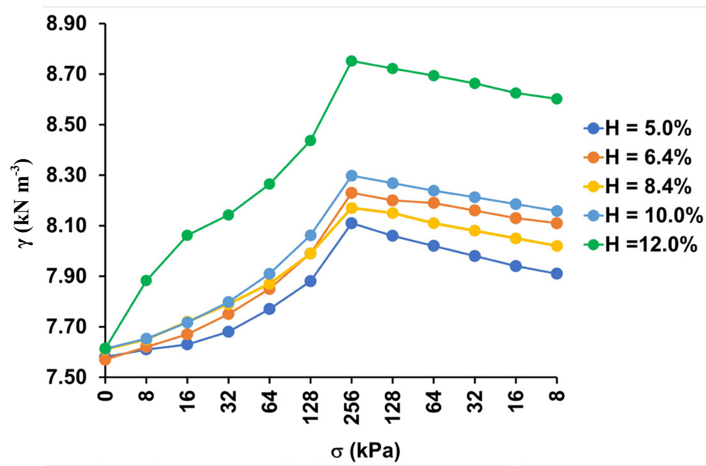

Fig. 11. Variation in apparent specific weight as a function of the applied normal stress for the moisture contents analysed.

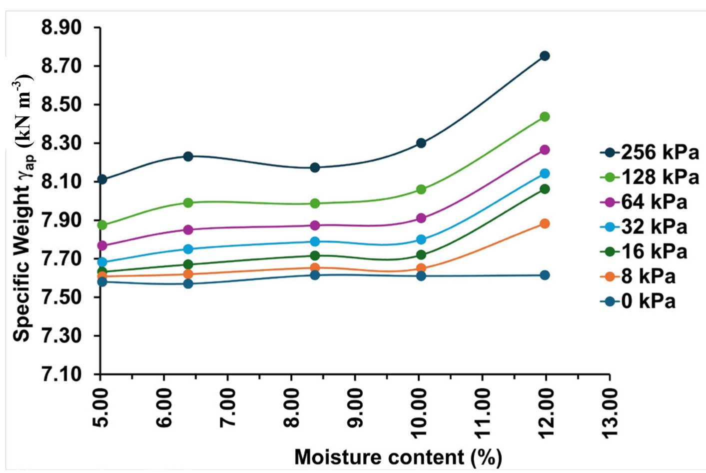

Fig. 12. Variation in apparent specific weight as a function of moisture content for different applied normal stresses.

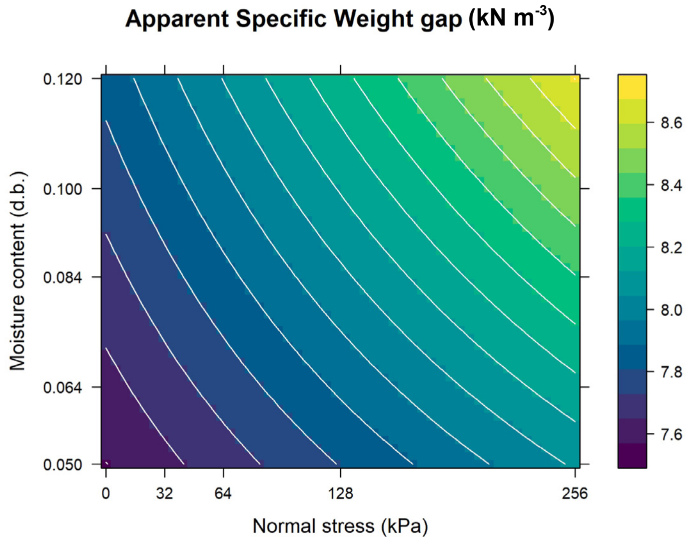

Fig. 13. Variation in apparent specific weight as a function of moisture content for different applied normal stresses, based on the fitted interaction model.

Table 8. Mean values and standard deviation of the apparent specific weight at each normal stress and moisture content applied in the oedometer tests conducted

Normal stress (kPa)	Apparent specific weight γ_{ap} (kN m^{-3}) Moisture content (d.b.)					Linear regression model	
	5.0%	6.4%	8.4%	10.0%	12.0%	$r_{pearson}$	p-value
0	7.58 ± 0.00	7.57 ± 0.01	7.61 ± 0.01	7.61 ± 0.01	7.61 ± 0.01	0.78	< 0.001
8	7.61 ± 0.02	7.62 ± 0.04	7.65 ± 0.01	7.65 ± 0.01	7.88 ± 0.03	0.82	< 0.001
16	7.63 ± 0.02	7.67 ± 0.05	7.72 ± 0.02	7.72 ± 0.02	8.06 ± 0.05	0.83	< 0.001
32	7.68 ± 0.03	7.75 ± 0.06	7.79 ± 0.05	7.80 ± 0.01	8.14 ± 0.04	0.84	< 0.001
64	7.77 ± 0.04	7.85 ± 0.08	7.87 ± 0.07	7.91 ± 0.03	8.26 ± 0.06	0.83	< 0.001
128	7.87 ± 0.01	7.99 ± 0.10	7.99 ± 0.11	8.06 ± 0.05	8.44 ± 0.08	0.83	< 0.001
256	8.11 ± 0.01	8.23 ± 0.10	8.17 ± 0.15	8.30 ± 0.08	8.75 ± 0.18	0.77	0.001
128	8.06 ± 0.03	8.20 ± 0.12	8.15 ± 0.16	8.27 ± 0.08	8.72 ± 0.18	0.77	0.001
64	8.02 ± 0.03	8.19 ± 0.11	8.11 ± 0.16	8.24 ± 0.07	8.69 ± 0.18	0.77	0.001
32	7.98 ± 0.02	8.16 ± 0.11	8.08 ± 0.15	8.21 ± 0.07	8.66 ± 0.17	0.78	0.001
16	7.94 ± 0.02	8.13 ± 0.11	8.05 ± 0.15	8.19 ± 0.07	8.63 ± 0.16	0.78	< 0.001
8	7.91 ± 0.01	8.11 ± 0.11	8.02 ± 0.15	8.16 ± 0.07	8.60 ± 0.15	0.79	< 0.001

Figure 13 illustrates the combined influence of moisture content and normal stress on the apparent specific weight.

Finally, Table 8 provides the mean values and standard deviation obtained for the apparent specific weight, depending on the applied normal stress and moisture content of the sample.

The analysis of the above data revealed that the greatest difference in apparent specific weight between the maximum and minimum values obtained within the specified range for each moisture content, under the various normal stresses applied, was 15.0% at a moisture content of 12.0%. This was followed by the value recorded at a moisture content of 10.0% (9.1%), whilst those obtained at moisture contents of 6.4, 8.4, and 5.0 were 8.7, 7.4, and 7.0%, respectively. Finally, the greatest difference between the various values provided in the table was 15.6%, corresponding to the difference between the maximum value of this parameter (8.75 kN m^{-3}), which was achieved at a moisture content of 12.0% and a normal stress of 256 kPa, and the minimum (7.57 kN m^{-3}), which corresponded to a moisture content of 6.4% and a normal stress of 0 kPa. The p-values obtained indicated that, during the loading cycle (0 to 256 kPa), the combined effect of moisture content and normal stress on apparent specific weight was statistically significant ($p < 0.001$), whereas this combined effect during the unloading cycle (256 to 0 kPa) was not significant ($p = 0.920$). Nevertheless, significant positive correlations between moisture content and apparent specific weight were observed at all normal stress levels during both loading and unloading cycles.

4. DISCUSSION

4.1. Moisture content

The range of values selected in this study for wood pellet samples regarding moisture content was within that used in other studies related to this material (Hartley and Wood, 2008; Lee *et al.*, 2020; Masche *et al.*, 2023; Sadeq *et al.*, 2023a; Wu *et al.*, 2011). Therefore, whenever possible, the results presented here will be compared with those reported in other studies.

Although the aim of this study was not to analyse in depth the influence of moisture content on the dimensions and geometry of individual wood pellet particles, these changes became evident as the moisture content increased. Thus, an increase of up to 3.5% in length was observed at the highest moisture level applied, whilst this percentage rose to 55% for the diameter. These results are consistent with those obtained by other authors (Sadeq *et al.*, 2023b), who observed that radial swelling is significantly greater than swelling in the longitudinal direction, whilst the variation in length was smaller than that reported in other studies (Dhamodaran and Afzal, 2012). Furthermore, other studies have examined the effects of the humidification process on individual wood pellets. Among these effects, those related to changes in the durability, volumetric swelling, and density of pellets are particularly noteworthy (Deng *et al.*, 2019; Lee *et al.*, 2021).

4.2. Direct shear tests

4.2.1. Angle of internal friction, effective angle of internal friction, and apparent cohesion

With regard to the direct shear tests carried out, the shape of the stress-strain curves obtained were smooth in shape and similar to those observed for other granular (Moya *et al.*, 2022; Przywara *et al.*, 2023; Stasiak *et al.*, 2015) or powdered (Ramírez *et al.*, 2010) materials.

The results obtained for the internal friction angle were similar to those found in other studies (Moya *et al.*, 2022; Wu *et al.*, 2011) or those found for moist wood powder (Barletta and Poletto, 2013) or sawdust (Miccio *et al.*, 2013). However, the minimum value obtained here (35.7º) was around 7% higher than the maximum reported for forest woodchips (Stasiak *et al.*, 2018), 18% higher than the maximum reported for pine pellets with a Jenike shear tester (Stasiak *et al.*, 2019), or 5 and 32% higher than those found for woodchips and sawdust, respectively (Stasiak *et al.*, 2015).

When analysing the results obtained for the angle of internal friction under low (13, 25, and 64 kPa) and high (125, 250, and 374 kPa) normal stresses, these were in line with those published for the same material by other authors (Wu *et al.*, 2011), as well as those corresponding to woodchips (Stasiak *et al.*, 2018, 2015), woody biomass powders (Barletta and Poletto, 2013), or sawdust and olive husk (Miccio *et al.*, 2013), whilst the minimum (32.6º) was 7.9% higher than the maximum recorded for pine biomass (Stasiak *et al.*, 2019).

Since pellets are densified products, the material they are made of is not particularly important; consequently, similar values for the angle of internal friction can be obtained in different studies using similar devices (Stasiak *et al.*, 2019).

As regards the values of the effective angle of internal friction, the range of values obtained here was within that found by other authors for wood pellets (Wu *et al.*, 2011) or other materials, such as sawdust or olive husk (Miccio *et al.*, 2013), whilst the minimum value obtained (38.6º) was in line with those provided for forest woodchips using a Jenike shear tester (Stasiak *et al.*, 2018, 2015). However, it was around 13.5% higher than that obtained for sawdust (Stasiak *et al.*, 2015), 5.5% higher than the maximum reported for pine biomass (Stasiak *et al.*, 2019), or 15.6% and 20% lower than those found for woody biomass powder (Barletta and Poletto, 2013) and dry sawdust (Miccio *et al.*, 2011), respectively.

Regarding the results obtained for the effective angle of internal friction under low and high normal stresses, most of these values fell within the range reported by other researchers for wood pellets (Wu *et al.*, 2011) or for other biomass products, such as woodchips (Stasiak *et al.*, 2018, 2015), woody biomass powders (Barletta and Poletto, 2013), sawdust (Miccio *et al.*, 2013, 2011), or olive husk (Miccio *et al.*, 2013). In other cases, these values were higher than those provided in other studies, *e.g.*, they were 12.6% higher than those found for pine biomass (Stasiak *et al.*, 2019).

Neither for the angle of internal friction nor for the effective angle of internal friction was any correlation detected between these parameters and the moisture content of the sample, which was consistent with findings in similar materials reported in other studies (Stasiak *et al.*, 2019) but differed from the findings for other materials, such as sawdust (Stasiak *et al.*, 2015) or woodchips (Stasiak *et al.*, 2018). Nevertheless, the combined effect of normal stress and moisture content on shear stress was significant, which was consistent with other studies (Stasiak *et al.*, 2019).

The causes of the relatively small differences found between the values provided in this study and those found in other studies may include the particle arrangement, moisture content, bulk density, shear banding, particle orientation within the shear box, particle shape, or consolidation time (Molenda and Horabik, 2005).

Regarding apparent cohesion, the values obtained for this parameter in the direct shear tests fell within the range reported for the same material under ambient conditions (Moya *et al.*, 2022), as well as within the values reported for woody biomass powders (Barletta and Poletto, 2013). However, these values were higher than those reported in other studies. Thus, the minimum value obtained here (13.36 kPa) was 2.73 times higher than the maximum (4.9 kPa) recorded for forest woodchips (Stasiak *et al.*, 2018), whilst it was approximately 84 times higher than that recorded for sawdust (Miccio *et al.*, 2013).

When analysing the values obtained for this parameter under low or high normal stresses alone, similar conclusions were reached when comparing them with the values reported in the aforementioned studies, coinciding with those provided for wood pellets under ambient conditions (Moya *et al.*, 2022) or with those for woody biomass powders (Barletta and Poletto, 2013). However, in this case, the minimum values were 7.42 kPa for the low normal stress range and 2.26 kPa for the high normal stress range, which were 51% higher and in line with those provided, respectively, for forest woodchips (Stasiak *et al.*, 2018), whilst they were 46 and 14 times higher, respectively, than those for sawdust (Miccio *et al.*, 2013).

As noted in the 'Results' section, the values obtained for apparent cohesion were not influenced by moisture content, which is consistent with the findings reported in other studies (Stasiak *et al.*, 2019, 2018).

The differences in the values obtained for this parameter could be due to the least squares adjustment carried out since a linear Coulomb yield locus was assumed, according to other studies (Barletta and Poletto, 2013; Schulze, 2021; Wu *et al.*, 2011).

Finally, it should be noted that the maximum normal stress applied in these tests (374 kPa) was well above the maximum typically reached in commercial silos, which is around 120-150 kPa. The reason for this overloading is to carry out tests that yield results under conditions similar to those used in previous studies with other materials using the circular shear cell (Moya *et al.*, 2006), which involves providing values for these parameters under extreme conditions. Clearly, when the material was subjected to such high loads, some slight fragmentation of the material was observed, resulting in the formation of some smaller particles and the fracture of larger ones. The amount of material that may have been damaged was not quantified, but in light of the results obtained, it can be stated that this did not significantly distort them, as it has been verified that they fall within the range of those published by other authors.

4.2.2. Dilatancy angle

Based on the direct shear tests carried out, the corresponding deformation curves were plotted, which in turn made it possible to determine the dilatancy angle values. The literature review on granular materials, and more specifically on biomass products, did not yield any information relevant to this study, except for a previous study conducted by the authors on wood pellets under ambient conditions (Moya *et al.*, 2022). The deformation curves obtained were similar to those found for granular agricultural materials (Moya *et al.*, 2013; Zeng *et al.*, 2020).

As noted in the 'Results' section, the maximum value (35.6º) was slightly lower (2.2%) than the maximum (36.4º) recorded for the same material under ambient conditions (Moya *et al.*, 2022). Although there were some exceptions, the general trend was that the higher the normal stress applied, the lower the dilatancy angle, in line with findings in the literature regarding wood pellets (Moya *et al.*, 2022) and other granular agricultural materials (Moya *et al.*, 2013; Moya-Ignacio *et al.*, 2024; Zeng *et al.*, 2020; Zeng and Wang, 2019). This is because the greater the normal stress applied, the softer the material becomes. Consequently, this softening makes the material easier to compress, particularly in the presence of water, thereby reducing dilatancy. Similar conclusions could be drawn for this parameter when direct shear tests were carried out using a modified shear box, although in this case a more irregular behaviour was observed with regard to the dependence of this parameter on the applied normal stress.

Finally, no correlation was observed between the dilatancy angle and the moisture content of the samples, as was the case when the angle of internal friction and the effective angle of internal friction were analysed.

4.2.3. Grain-wall friction

The direct shear tests using a modified shear box allowed obtaining the coefficient of grain-wall friction, the coefficient of effective grain-wall friction, and their corresponding angles, as noted in the 'Results section'. The results obtained showed that the minimum value for the grain-wall friction coefficient was 0.51 (27.0º), which was 2.2% lower than the value provided for the same material (0.52) under ambient conditions (Moya *et al.*, 2022), 28.6% greater than the maximum (21º) reported for wood pellets using stainless steel, and 22.7% greater than the maximum (22º) provided for mild steel (Wu *et al.*, 2011), as well as 45% greater than that reported for wood pellet particles (18.62º) in another study (Gallego *et al.*, 2020). As regards the values of the coefficient of effective grain-wall friction, these could not be compared with those of similar products since no data have been reported in the literature.

With regard to the values of the grain-wall friction coefficient obtained under low and high normal stresses, the minimum value recorded under low normal stresses (0.51) was similar to that provided for wood pellets under ambient conditions (Moya *et al.*, 2022), and the corresponding angle (27.2º) was 29.5% and 23.6% higher than those reported by other authors (Wu *et al.*, 2011) for stainless steel and mild steel, respectively, or 46.2% higher than that recorded for wood pellet particles (Gallego *et al.*, 2020). Similarly, when considering only the values obtained for this parameter under high normal stresses, the minimum value (0.42) was 17.6% lower than that recorded under ambient conditions (Moya *et al.*, 2022), whilst it was 7.6 and 2.7% higher than those reported for stainless steel and mild steel, respectively (Wu *et al.*, 2011) and 21.5% higher than that reported for wood pellet particles (Gallego *et al.*, 2020). Again, as expected, no correlation was detected between the grain-wall friction coefficients and the moisture content for either low or high normal stresses.

4.3. Oedometer tests

The range of values obtained for the apparent specific weight using the oedometer devices varied between 7.57 kN m^{-3}, when no normal stress was applied, and 8.75 kN m^{-3}, for a normal stress of 256 kPa. Therefore, the minimum value was in line with the range suggested in other studies (Alakangas *et al.*, 2007); it was 6.9% higher than the minimum recorded for the same material (7.08 kN m^{-3}) under ambient conditions (Moya *et al.*, 2022) and around 43% higher than the minimum (5.20 and 5.28 kN m^{-3}) recorded for wood pellets (Obernberger and Thek, 2004; Wu *et al.*, 2011), respectively, whilst the maximum was 22.7, 36.7, and 34.8% higher than the maximum (7.13, 6.40, and 6.28 kN m^{-3}) reported in the last three studies, respectively. These differences may have been due to the equipment used to carry out these tests. In this study, the authors used an oedometer cell 75 mm in diameter and 20 mm in height, whilst the authors of the other studies used a standard Proctor mould 102 mm in diameter and 122 mm in height (Moya *et al.*, 2022), a graduated cylinder (Obernberger and Thek, 2004), and a steel pan and a 1 l steel can (Wu *et al.*, 2011), respectively.

Based on the various tests carried out, it was observed that, as a general trend, the higher the moisture content of the sample, the higher the apparent specific weight at all normal stress levels during both loading and unloading cycles. However, there was an exception when a moisture content of 6.4% was applied, as explained in the 'Results' section. This was consistent with the trends considered in other studies (Wu *et al.*, 2011), although it was the opposite of what was observed in other studies involving different types of biomass such as SRF poplar and corn stover (Gil *et al.*, 2013) or pecan shells (Littlefield *et al.*, 2011). The arrangement of the wood pellet particles within the oedometric cell, as well as their orientation in the presence of water, may have influenced the results presented in this study.

The behaviour of the material, both at rest, when stored, and in motion, when flowing, depends to a large extent on the mechanical properties analysed in this study (Chen *et al.*, 2023; Miccio *et al.*, 2013). These properties depend largely on certain factors, such as moisture content of the material, temperature, relative humidity, etc. The properties determined in this study are important because they could provide information regarding the mechanical strength of wood pellets. A decrease in mechanical strength can influence the generation of dust and fine particles (Gilvari *et al.*, 2020). Furthermore, these properties influence the stresses and torques generated during the emptying of silos using screw feeders. Determining the torques allows an estimate of the material's resistance to loads during storage and to flow disruption during discharge (Stasiak *et al.*, 2019). Furthermore, these forces may arise during the discharge of densified products from screw feeders into silos, or from silos or trucks onto the ground, which determine the impact resistance. In such cases, it is important to calculate the safety height in pellet production (Kaliyan and Vance Morey, 2009). Finally, the environmental conditions often vary and affect pellets. Exposure to rain or changes in temperature or relative humidity during the transportation and storage of densified products, such as pellets, can affect both their physical and mechanical properties (Kaliyan and Vance Morey, 2009). Among these changes, bulk density may be altered, which in turn affects other mechanical properties. For this reason, it is essential to understand these factors in order to design suitable, efficient, and cost-effective facilities and infrastructure for the handling and storage of these biomass materials.

Finally, by way of a concluding remark, it should be noted that the direct shear tests were carried out using a circular shear box 100 mm in diameter, as explained in the 'Materials and Methods' section. As indicated, the ratio between the diameter of the shear cell and the maximum particle size is far from that recommended in Eurocode 1, Part 4 (UNE-EN-1991-4:2011/AC, 2013). Therefore, the results provided in this study regarding the parameters obtained from the tests carried out with this device are subject to a scale effect. Thus, according to several studies conducted on different soil types (Ahmad *et al.*, 2025; Cerato and Lutenegger, 2006; Li *et al.*, 2022; Wu *et al.*, 2008), higher friction angles and lower cohesion are obtained at lower values of the ratio between particle size and box size. Consequently, the angle of friction decreases and cohesion increases as the size of the shear box is larger. Various factors may influence this trend. Among these, it is worth noting that interparticle locking may be reduced when larger shear boxes are used, which decreases the measured friction angle (Li *et al.*, 2022; Wu *et al.*, 2008). Furthermore, larger shear boxes have a wider shear plane, which facilitates the rearrangement of larger particles and dilation, which, in turn, can dissipate shear strength, reducing peak friction values (Cantor and Ovalle, 2025).

With regard to apparent cohesion, in large specimens there may be more particles spanning the shear plane, allowing the formation of localised bridging or interlocking effects, which can simulate apparent cohesion in granular materials. Furthermore, in larger boxes, boundary effects may arise, such as those attributed to friction between the material mass and the walls of the shear box, which increases the measured cohesion (Deiminiat and Li, 2022).

It is also important to consider the influence of relative density. Several studies (Ahmad *et al.*, 2025; Cerato and Lutenegger, 2006) have concluded that an increase in relative density increases the angle of friction. However, when the density remains constant, the larger the box size, the lower the friction angle. Therefore, when density influences shear strength, scale effects are significant (Ahmad *et al.*, 2025).

With respect to the dilatancy angle, it has been shown that, in the case of granular materials, this parameter decreases significantly as the mean particle size, D_{50}, increases (Amirpour Harehdasht *et al.*, 2019; Harehdasht *et al.*, 2017). Furthermore, the larger the size of the shear box used, the smaller the dilatancy angle obtained (Cui and O'Sullivan, 2006) due to the same factors already discussed above for parameters dependent on shear strength.

As for the grain-wall friction coefficient, the size of the shear box used influences the value of the interface friction angle obtained. In recent studies (Bauer and Ebrahimian, 2021), it was observed that the maximum mobilised interface friction angle increases as the box length decreases. Therefore, this parameter is slightly higher for the smaller shear box. Furthermore, the scale effect may result in an average interface friction angle lower than the prescribed value.

For these reasons, the values provided in this study should be regarded as merely indicative for the design of silos, as the scale effect may lead to some discrepancies between the calculated parameters and the actual values.

5. CONCLUSIONS

The values of the angle of internal friction ranged from 35.7º to 41.4º, which were similar to those reported in other studies for wood pellets and to those found for moist wood powder or sawdust, but higher than those reported for other materials such as pine pellets or forest woodchips.

No correlation was found between the moisture content of the sample and the parameters relating to the angle of internal friction, the effective angle of internal friction, the apparent cohesion, the dilatancy angle, or the grain-wall friction coefficient. This result was consistent with those found in other studies involving similar materials, but differed from those observed with other materials, such as sawdust or woodchips.

From the normal direct shear tests carried out, it was observed that the combined effect of normal stress and moisture content presented a significant interaction on shear stress ($p = 0.011$).

The values obtained for the apparent cohesion ranged from 13.36 to 22.66 kPa, which were in line with those reported for wood pellets under ambient conditions and for woody biomass powders, although they were higher than those reported for other materials such as forest woodchips or sawdust.

Based on the tests carried out in this study, it could be observed that, as a general trend, the higher the normal stress applied, the lower the dilatancy angle, which was in line with other studies for wood pellets as well as for granular agricultural materials.

A correlation was detected between the moisture content of the sample and the apparent specific weight at all normal stress levels, which was consistent with some studies carried out with wood pellets but differed from what was observed with other different types of biomass, such as SRF poplar, corn stover, or pecan-shells.

Although not quantified, the application of high normal stresses in the direct shear tests caused slight fragmentation of the material, resulting in the formation of some smaller particles and the fracture of larger ones. In any case, this did not significantly distort the results obtained in this study, as they fall within the range of values reported by other authors.

Changes in the dimensions and geometry of the wood pellet particles were observed during the humidification process. These changes became apparent as the moisture content increased. Radial swelling was significantly greater than swelling in the longitudinal direction, which is consistent with findings in other studies.

The values provided in this study should be considered merely indicative for silo design, as the scale effect may lead to some discrepancies between the calculated parameters and the actual values.

It is essential to understand the various parameters set out in this study to design suitable, efficient, and cost-effective facilities and infrastructure for the handling and storage of biomass products.

Authors contributions: Research concept and design: M.M.I., J.R.V.G.; Collection and/or assembly of data: M.M.I., M.C.G.; Data analysis and interpretation: M.M.I., J.R.V.G., P.V.L., M.C.G.; Writing the article: M.M.I.; Critical revision of the article: M.M.I., J.R.V.G., P.V.L., M.C.G.; Final approval of the article: M.M.I., J.R.V.G., P.V.L., M.C.G. All authors have read and agreed to the published version of the manuscript.

Conflict of interest: The authors declare that they have no known competing financial interests or personal relationships that could have appeared to influence the work reported in this paper.

6. REFERENCES

Ahmad, I., Rehman, Z., Junaid Iqbal, M., Rehman, W., 2025. The scale direct shear test effect on the shear strength characteristics of different sands in Lahore, Pakistan. Asian J. Sci. Eng. Technol. (AJSET) 4, 13-25. https://doi.org/10.47264/idea.ajset/4.2.2

Alakangas, E., Heikkinen, A., Lensu, T., Vesterinen, P., 2007. Biomass fuel trade in Europe Summary Report VTT-R-03508-07.

Amirpour Harehdasht, S., Hussien, M.N., Karray, M., Roubtsova, V., Chekired, M., 2019. Influence of particle size and gradation on shear strength-dilation relation of granular materials. Canadian Geotechnical J. 56, 208-227. https://doi.org/10.1139/cgj-2017-0468

Bagherzadeh Kh., A., Mirghasemi, A.A., Mohammadi, S., 2011. Numerical simulation of particle breakage of angular particles using combined DEM and FEM. Powder Technol. 205, 15-29. https://doi.org/10.1016/j.powtec.2010.07.034

Barletta, D., Poletto, M., 2013. An assessment on silo design procedures for granular woody biomass. Chem. Eng. Trans. 32, 2209-2214.

Bauer, E., Ebrahimian, B., 2021. Investigations of granular specimen size effect in interface shear box test using a micro-polar continuum description. Int. J. Numer. Anal. Methods Geomech. 45, 2467-2489. https://doi.org/10.1002/nag.3273

Bhise, S., Kaur, A., Manikantan, M., 2014. Moisture dependent physical properties of maize (PMH-1). Acta Aliment. 43, 394-401. https://doi.org/10.1556/AAlim.43.2014.3.5

Cantor, D., Ovalle, C., 2025. Sample size effects on the critical state shear strength of granular materials with varied gradation and the role of column-like local structures. Géotechnique 75, 29-40. https://doi.org/10.1680/jgeot.23.00032

Çarman, K., 1996. Some physical properties of lentil seeds. J. Agric. Engng. Res. 63, 87-92. https://doi.org/10.1006/jaer.1996.0010

Cerato, A.B., Lutenegger, A.J., 2006. Specimen size and scale effects of direct shear box tests of sands. Geotechnical Testing J. 29. https://doi.org/10.1520/GTJ100312

Chandio, F.A., Li, Y., Ma, Z., Ahmad, F., Syed, T.N., Shaikh, S.A., *et al.*, 2021. Influences of moisture content and compressive loading speed on the mechanical properties of maize grain orientations. Int. J. Agric. Biological Eng. 14, 41-49. https://doi.org/10.25165/j.ijabe.20211405.6072

Chen, F., Xia, Y., Klinger, J., Chen, Q., 2023. Hopper discharge flow dynamics of milled pine and prediction of process upsets using the discrete element method. Powder Technol. 415. https://doi.org/10.1016/j.powtec.2022.118165

Chen, Z., Wassgren, C., Veikle, E., Ambrose, K., 2020. Determination of material and interaction properties of maize and wheat kernels for DEM simulation. Biosyst. Eng. 195, 208-226. https://doi.org/10.1016/j.biosystemseng.2020.05.007

Cheng, X., Zhang, Q., Shi, C., Yan, X., 2017. Model for the prediction of grain density and pressure distribution in hopper-bottom silos. Biosyst. Eng. 163, 159-166. https://doi.org/10.1016/j.biosystemseng.2017.09.006

Cui, L., O'Sullivan, C., 2006. Exploring the macro-and micro-scale response of an idealised granular material in the direct shear apparatus. Géotechnique 56, 455-468. https://doi.org/10.1680/geot.2006.56.7.455

Davies, R.M., El-Okene, A.M., 2009. Moisture-dependent physical properties of soybeans. Int. Agrophys. 23, 299-303.

Deiminiat, A., Li, L., 2022. Experimental study on the reliability of scaling down techniques used in direct shear tests to determine the shear strength of rockfill and waste rocks. CivilEng 3, 35-50. https://doi.org/10.3390/civileng3010003

Deng, T., Alzahrani, A.M., Bradley, M.S., 2019. Influences of environmental humidity on physical properties and attrition of wood pellets. Fuel Processing Technol. 185, 126-138. https://doi.org/10.1016/j.fuproc.2018.12.010

Dhamodaran, A., Afzal, M.T., 2012. Springback in pellets. Bioresources 7, 4362-4376. https://doi.org/10.15376/biores.7.3.4362-4376

Doerich, C., Rotter, J., 2011. Accurate determination of plastic collapse loads from finite element analyses. J. Pressure Vessel Technol. 133, 011202-011202-10. https://doi.org/10.1115/1.4002770

EN ISO 17225-1, 2022. Solid biofuels. Fuel specifications and classes. Part 1: General requirements].

ENplus, 2023. ENplus® GD 3001:2023. Storage for Wood Pellets. Brussels, Belgium.

Flach, B., Bolla, S., 2025. Wood pellets annual. European Union. please add more information about editor, city, country.

Gallego, E., Fuentes, J.M., Ruiz, Á., Hernández-Rodrigo, G., Aguado, P., Ayuga, F., 2020. Determination of mechanical properties for wood pellets used in DEM simulations. Int. Agrophys. 34, 485-494. https://doi.org/10.31545/intagr/130634

Gallego, E., Madrid, M., Fuentes, J.M., Wiącek, J., Grande, A., Ayuga, F., 2025. DEM analysis of friction of cylindrical pinewood pellets with corrugated steel silo walls. Comput. Part. Mech. 12, 2081-2100. https://doi.org/10.1007/s40571-025-00906-3

Ganesan, V., Rosentrater, K.A., Muthukumarappan, K., 2008. Flowability and handling characteristics of bulk solids and powders – a review with implications for DDGS. Biosyst. Eng. 101, 425-435. https://doi.org/10.1016/j.biosystemseng.2008.09.008

Gao, M., Cheng, X., Du, X., 2018. Simulation of bulk density distribution of wheat in silos by finite element analysis. J. Stored Prod. Res. 77, 1-8. https://doi.org/10.1016/j.jspr.2018.02.003

Gierz, Ł., Kolankowska, E., Markowski, P., Koszela, K., 2022. Measurements and analysis of the physical properties of cereal seeds depending on their moisture content to improve the accuracy of DEM simulation. Appl. Sci. (Switzerland) 12. https://doi.org/10.3390/app12020549

Gil, M., Schott, D., Arauzo, I., Teruel, E., 2013. Handling behavior of two milled biomass: SRF poplar and corn stover. Fuel Processing Technol. 112, 76-85. https://doi.org/10.1016/j.fuproc.2013.02.024

Gilvari, H., Cutz, L., Tiringer, U., Mol, A., de Jong, W., Schott, D.L., 2020. The effect of environmental conditions on the degradation behavior of biomass pellets. Polymers (Basel). 12. https://doi.org/10.3390/polym12040970

Harehdasht, S.A., Karray, M., Hussien, M.N., Chekired, M., 2017. Influence of particle size and gradation on the stress-dilatancy behavior of granular materials during drained triaxial compression. Int. J. Geomechanics 17. https://doi.org/10.1061/(ASCE)GM.1943-5622.0000951

Härtl, J., Ooi, J.Y., 2011. Numerical investigation of particle shape and particle friction on limiting bulk friction in direct shear tests and comparison with experiments. Powder Technol. 212, 231-239. https://doi.org/10.1016/j.powtec.2011.05.022

Hartley, I.D., Wood, L.J., 2008. Hygroscopic properties of densified softwood pellets. Biomass Bioenergy 32, 90-93. https://doi.org/10.1016/j.biombioe.2007.06.009

Hilal, A., Sanad, A.M., Abdelbarr, M.H., Ramadan, O.M.O., Abdalla, H.A., 2022. Three-dimensional finite element analysis for pressure on flexible wall silos. Appl. Sci. (Switzerland) 12. https://doi.org/10.3390/app12189251

Horabik, J., Bańda, M., Józefaciuk, G., Adamczuk, A., Polakowski, C., Stasiak, *et al.*, 2021. Breakage strength of wood sawdust pellets: Measurements and modelling. Materials 14. https://doi.org/10.3390/ma14123273

International Energy Agency, I., 2025. Renewables 2025. Analysis and forecasts to 2030, Biomass and Bioenergy.

Izli, N., Unal, H., Sincik, M., 2009. Physical and mechanical properties of rapeseed at different moisture content. Int. Agrophys. 23, 137-145.

Janssen, H., 1895. Versuche über Getreidebruck in Silozellen. Zeitschrift des Vereines deutscher Ingenieure 1045-1049.

Jofriet, J.C., Lelievre, B., Fwa, T.F., 1977. Friction model for finite element analyses of silos. Trans. Am. Soc. Agric. Eng. 735-740.

Kaliyan, N., Vance Morey, R., 2009. Factors affecting strength and durability of densified biomass products. Biomass Bioenergy 33, 337-359. https://doi.org/10.1016/j.biombioe.2008.08.005

Kibar, H., 2017. Patterns between wall pressures and stresses with grain moisture on cylindrical silo. Structural Eng. Mechanics 62, 487-496. https://doi.org/10.12989/sem.2017.62.4.487

Kibar, H., Öztürk, T., 2008. Physical and mechanical properties of soybean. Int. Agrophys. 22, 239-244.

Kobyłka, R., Molenda, M., Horabik, J., 2019. Loads on grain silo insert discs, cones, and cylinders: Experiment and DEM analysis. Powder Technol. 343, 521-532. https://doi.org/10.1016/j.powtec.2018.11.032

Kruszelnicka, W., Chen, Z., Ambrose, K., 2022a. Moisture-dependent physical-mechanical properties of maize, rice, and soybeans as related to handling and processing. Materials 15. https://doi.org/10.3390/ma15248729

Kruszelnicka, W., Diviš, J., Hlosta, J., Gierz, Ł., Žurovec, D., 2022b. Calibration of selected bulk biomaterials parameters for dem simulation of comminution process. Case Study - Corn and Rice Grains. Advances Sci. Technol. Res. J. 16, 64-77. https://doi.org/10.12913/22998624/15 2990

Kruszelnicka, W., Leda, P., Tomporowski, A., Ambrose, K., 2024. Breakage behavior of corn kernels subjected to repeated loadings. Powder Technol. 435. https://doi.org/10.1016/j.powtec.2024.119372

Lebègue, Y., Boudakian, A., 1989. Bases des règles silos du SNBATI-Essais sur les produits et principes des formules silos. Ann. ITBTP 69-113.

Lee, J.S., Sokhansanj, S., Lau, A.K., Lim, C.J., 2020. Physical properties of wood pellets exposed to liquid water. Biomass Bioenergy 142. https://doi.org/10.1016/j.biombioe.2020.105748

Lee, J.S., Sokhansanj, S., Lau, A.K., Lim, J., Bi, X.T., 2021. Moisture adsorption rate and durability of commercial softwood pellets in a humid environment. Biosyst. Eng. 203, 1-8. https://doi.org/10.1016/j.biosystemseng.2020.12.011

Li, S., Wang, T., Wang, H., Jiang, M., Zhu, J., 2022. Experimental studies of scale effect on the shear strength of coarse-grained soil. Appl. Sci. (Switzerland) 12. https://doi.org/10.3390/app12010447

Littlefield, B., Fasina, O.O., Shaw, J., Adhikari, S., Via, B., 2011. Physical and flow properties of pecan shells-particle size and moisture effects. Powder Technol. 212, 173-180. https://doi.org/10.1016/j.powtec.2011.05.011

Liu, Y., Liu, H., Mao, H., 2017. DEM investigation of the effect of intermediate principle stress on particle breakage of granular materials. Comput. Geotech. 84, 58-67. https://doi.org/10.1016/j.compgeo.2016.11.020

Lopes Neto, J.P., do Nascimento, J.W.B., Marques, J.I., da Costa, C.A., 2016. Mechanical properties of grain in silos for simulation designs. Engenharia Agricola 36, 573-580. https://doi.org/10.1590/1809-4430-Eng.Agric.v36n4p573-580/2016

Lu, Y., Jin, W., Klinger, J.L., Dai, S., 2023. Effects of the moisture content on the flow behavior of milled woody biomass. ACS Sustain. Chem. Eng. 11, 11482-11489. https://doi.org/10.1021/acssuschemeng.3c01344

Markauskas, D., Ramírez-Gómez, Á., Kačianauskas, R., Zdancevičius, E., 2015. Maize grain shape approaches for DEM modelling. Comput. Electron. Agric. 118, 247-258. https://doi.org/10.1016/j.compag.2015.09.004

Masche, M., Puig-Arnavat, M., Jensen, P.A., Holm, J.K., Clausen, S., Ahrenfeldt, J., *et al.*, 2023. Influence of wood pellets properties on their grinding performance. Biomass Convers. Biorefin. 2985-3000. https://doi.org/10.1007/s13399-021-01559-x

Miccio, F., Barletta, D., Poletto, M., 2013. Flow properties and arching behavior of biomass particulate solids. Powder Technol. 235, 312-321. https://doi.org/10.1016/j.powtec.2012.10.047

Miccio, F., Silvestri, N., Barletta, D., Poletto, M., 2011. Characterization woody biomass flowability. Chem. Eng. Trans. 24, 643-648.

Mohammad, Z., Anwar, M., Ansari, S.S., Baqi, A., 2023. Finite element modelling of rc silo subjected to thermal loads. In: Lecture Notes in Civil Engineering. Springer Science and Business Media Deutschland GmbH, 419-427. https://doi.org/10.1007/978-981-19-4055-2_33

Molenda, M., Horabik, J., 2005. Mechanical properties of granular agro-materials and food powders for industrial practice. Part I: characterization of mechanical properties of particulate solids for storage and handling. Institute of Agrophysics Polish Academy of Science, Lublin, Poland. https://doi.org/10.13140/2.1.2810.1447

Molenda, M., Horabik, J., Łukaszuk, J., Wiacek, J., 2011. Variability of intergranular friction and its role in DEM simulation of direct shear of an assembly of rapeseeds. Int. Agrophys. 25, 361-368.

Moya, M., Aguado, P.J., Ayuga, F., 2013. Mechanical properties of some granular agricultural materials used in silo design. Int. Agrophys. 27, 181-193. https://doi.org/10.2478/v10247-012-0084-9

Moya, M., Guaita, M., Aguado, P., Ayuga, F., 2006. Mechanical properties of granular agricultural materials, part 2. Trans. ASABE 49, 479-489. https://doi.org/10.13031/2013.20403

Moya, M., Sánchez, D., Romero, J.Á., Villar-García, J.R., 2024. Influence of moisture content on some mechanical properties of wheat. Agronomy 14. https://doi.org/10.20944/preprints202401.1241.v1

Moya, M., Sánchez, D., Villar-García, J.R., 2022. Values for the mechanical properties of wheat, maize and wood pellets for use in silo load calculations involving numerical methods. Agronomy 12. https://doi.org/10.3390/agronomy12061261

Moya-Ignacio, M., Sánchez, D., Romero, J.Á., Villar-García, J.R., 2024. Study of various mechanical properties of maize (*Zea mays*) as influenced by moisture content. Agronomy 14. https://doi.org/10.3390/agronomy14081613

Obernberger, I., Thek, G., 2004. Physical characterisation and chemical composition of densified biomass fuels with regard to their combustion behaviour. Biomass Bioenergy 27, 653-669. https://doi.org/10.1016/j.biombioe.2003.07.006

Przywara, M., Lech-Przywara, R., Zapała, W., Opaliński, I., 2023. Mechanical properties of solid biomass as affected by moisture content. AgriEngineering 5, 1118-1135. https://doi.org/10.3390/agriengineering5030071

Ramaj, I., Romuli, S., Schock, S., Müller, J., 2024. Discrete element modelling of bulk behaviour of wheat (*Triticum aestivum* L.) cv. 'Pionier' during compressive loading. Biosyst. Eng. 242, 123-139. https://doi.org/10.1016/j.biosystemseng.2024.04.005

Ramírez, A., Moya, M., Ayuga, F., 2010. Determination of the mechanical properties of powdered agricultural products and sugar. Particle and Particle Systems Characterization 26, 220-230. https://doi.org/10.1002/ppsc.200800016

Reimbert, M., Reimbert, A., 1987. Silos. Theory and Practice. Lavoisier.

Richefeu, V., Saïd, M., Youssoufi, E., Radjai, F., Farhang, R., Sa¨ıd, M., *et al.*, 2006. Shear strength properties of wet granular materials. Phys. Rev. E Stat. Nonlin. Soft Matter Phys. 73. https://doi.org/10.1103/PhysRevE.73.051304

Rotter, J.M., Holst, J.M.F.G., Ooi, J.Y., Sanad, A.M., 1998. Silo pressure predictions using discrete-element and finite-element analyses. Philosophical Transactions of the Royal Society A: Mathematical, Physical and Engineering Sciences 356, 2685-2712. https://doi.org/10.1098/rsta.1998.0293

Sadeq, A., Frank, A., Tyslik, M., Jägers, J., Pietsch-Braune, S., Scherer, V., *et al.*, 2023a. Influence of cyclic water content changes during long-term storage on the mechanical stability of wood pellets. Powder Technol. 428. https://doi.org/10.1016/j.powtec.2023.118866

Sadeq, A., Heinrich, D., Pietsch-Braune, S., Heinrich, S., 2023b. Influence of oscillating water content on the structure of biomass pellets. Powder Technol. 426. https://doi.org/10.1016/j.powtec.2023.118631

Sarnavi, H.J., Noor Mohammadi, A., Modares Motlagh, A., Rahmani Didar, A., 2013. DEM model of wheat grains in storage considering the effect of moisture content in direct shear test. Research J. Appl. Sci. Eng. Technol. 5, 829-841. https://doi.org/10.19026/rjaset.5.5029

Schulze, D., 2021. Powders and Bulk Solids. Springer Int. Publ. Cham. https://doi.org/10.1007/978-3-030-76720-4

Smith, R.M., Litster, J.D., 2012. Examining the failure modes of wet granular materials using dynamic diametrical compression. Powder Technol. 224, 189-195. https://doi.org/10.1016/j.powtec.2012.02.053

Stasiak, M., Molenda, M., Bańda, M., Gondek, E., 2015. Mechanical properties of sawdust and woodchips. Fuel 159, 900-908. https://doi.org/10.1016/j.fuel.2015.07.044

Stasiak, M., Molenda, M., Bańda, M., Wiącek, J., Parafiniuk, P., Lisowski, A., *et al.*, 2019. Mechanical characteristics of pine biomass of different sizes and shapes. European J. Wood Wood Products 77, 593-608. https://doi.org/10.1007/s00107-019-01415-w

Stasiak, M., Molenda, M., Gancarz, M., Wiącek, J., Parafiniuk, P., Lisowski, A., 2018. Characterization of shear behaviour in consolidated granular biomass. Powder Technol. 327, 120-127. https://doi.org/10.1016/j.powtec.2017.12.037

Stelte, W., 2012. Guideline: Storage and Handling of Wood Pellets.

Tabatabaeefar, A., 2003. Moisture-dependent physical properties of wheat. Int. Agrophys. 17, 207-211.

Thompson, S.A., Bucklin, R.A., Batich, C.D., 1988. Variation in the apparent coefficient of friction of wheat on galvanized steel. Trans. Am. Soc. Agric. Eng. 31, 1518-1524. https://doi.org/10.13031/2013.30894

Tumuluru, J.S., 2016. Specific energy consumption and quality of wood pellets produced using high-moisture lodgepole pine grind in a flat die pellet mill. Chemical Eng. Res. Design 110, 82-97. https://doi.org/10.1016/j.cherd.2016.04.007

UNE-EN ISO 17225-1, 2022. Solid biofuels. Fuel specifications and classes. Part 1: General requirements (in Spanish). (ISO 17225-1:2021).

UNE-EN ISO 17225-2, 2021. Solid biofuels. Fuel specifications and classes Part 2: Graded wood pellets (ISO 17225-2:2021). Madrid, Spain.

UNE-EN ISO 17892-1, 2015. Geotechnical investigation and testing. Laboratory testing of soil. Part 1: determination of water content.

UNE-EN ISO 17892-5, 2017. Geotechnical investigation and testing. Laboratory testing of soil. Part 5: incremental loading oedometer test.

UNE-EN ISO 17892-10, 2018. Geotechnical investigation and testing. Laboratory testing of soil. Part 10: Direct shear tests.

UNE-EN-1991-4:2011/AC, 2013. Eurocode 1: Actions on structures. Part 4: Silos and tanks.

United Nations Economic Commission for Europe (UNECE), 2025. Committee on Forests and the Forest Industry Forest Products Market.

United Nations Environment Programme, 2024. No more hot air … please! With a massive gap between rhetoric and reality, countries draft new climate commitments.

Weinhart, T., Labra, C., Luding, S., Ooi, J.Y., 2016. Influence of coarse-graining parameters on the analysis of DEM simulations of silo flow. Powder Technol. 293, 138-148. https://doi.org/10.1016/j.powtec.2015.11.052

Wiącek, J., Parafiniuk, P., Molenda, M., Horabik, J., Gallego, E., 2023. DEM study of microstructural effects in friction of wheat on corrugated steel surface. Tribol. Int. 183. https://doi.org/10.1016/j.triboint.2023.108435

Wu, M.R., Schott, D.L., Lodewijks, G., 2011. Physical properties of solid biomass. Biomass Bioenergy 35, 2093-2105. https://doi.org/10.1016/j.biombioe.2011.02.020

Wu, P.-K., Matsushima, K., Tatsuoka, F., 2008. Effects of specimen size and some other factors on the strength and deformation of granular soil in direct shear tests. Geotechnical Testing J. 31. https://doi.org/10.1520/GTJ100773

Zeng, C., Gu, H., Wang, Y., 2020. Stress-strain response of sheared wheat granular material stored in silos using triaxial compression tests. Int. Agrophys. 34, 103-114. https://doi.org/10.31545/intagr/116091

Zeng, C., Wang, Y., 2019. The shear strength and dilatancy behavior of wheat stored in silos. Complexity 2019. https://doi.org/10.1155/2019/1547616

Zheng, Z., Zang, M., Chen, S., Zhao, C., 2017. An improved 3D DEM-FEM contact detection algorithm for the interaction simulations between particles and structures. Powder Technol. 305, 308-322. https://doi.org/10.1016/j.powtec.2016.09.076

Zhu, X., Chi, R., Ma, Y., 2023. Effects of corn varieties and moisture content on mechanical properties of corn. Agronomy 13. https://doi.org/10.3390/agronomy13020545